High Strength Steels Treated by Quenching and Partitioning Process

X. J. Jin*, T. Y. Hsu, Y. H. Rong, X. D. Wang
H. P. Liu, H. Y. Li, Y. Wang, R. M. Wu, X. W. Lu
School of Materials Science and Engineering
Shanghai Jiao Tong University, 800 Dongchuan Rd, Shanghai 200240, China
*Email: jin@sjtu.edu.cn

L. Wang
Baosteel Research and Development Technology Center, Shanghai 201900, China

H. Dong, J. Shi
National Engineering Research Center of Advanced Steel Technology (NERCAST), Central Iron and Steel Research Institute (CISRI), Beijing 100081, China

J. F. Wang, X. C. Xiong
General Motor Shanghai Science Lab, Shanghai, China

National Science Foundation of China
National Basic Research Program of China (973 programs No. 2010 CB630800)

June 28@ University of Cambridge, UK

Location and Figures

Shanghai Jiao Tong University

40,275	Total number of students
18,000	Graduate students
18,275	Undergraduates
4,000	International students
2912	Full-time Faculty
687	Full professors
1039	Associate Professors
15	Academicians of Chinese Academy of Sciences
18	Academicians of Chinese Academy of Engineering
9	Lead Scientists of the National 973 Programs
44	National “Changjiang” Chair Professors
38	Recipients of National Science Funds for Outstanding Junior Faculty

For 2010

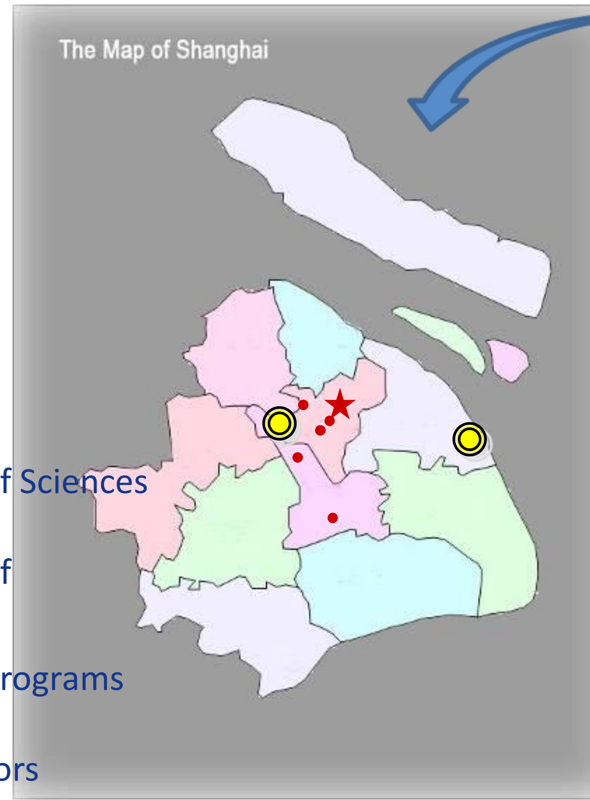

Nov. 17, 2010 Harry@SJTU

OUTLINE

- **Introduction**
- Quenching and Partitioning Treatment
  - Processing and Alloying
  - Microstructure and properties
  - Competing Process and Kinetics Models
    - Carbide formation and suppression
    - Migration of the martensite/austenite interface
    - Carbon partitioning and partitioning kinetics
- Combination of QPT with Hot Stamping and Application Concerns
- Unresolved Issues
- Concluding remarks

More steel is used than all other metals combined

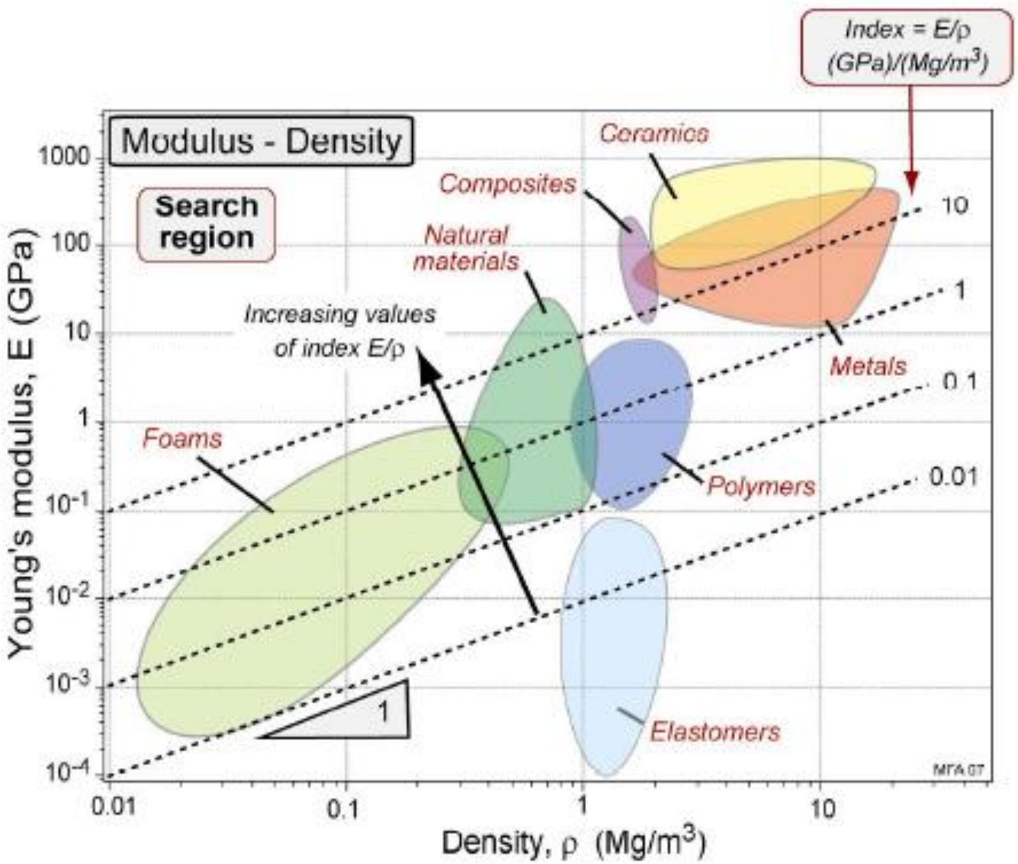

"Steel is strong, tough, easily formed and cheap. Its uses range from ships to paper clips. More steel is used than all other metals combined".

M. F. Ashby, D. Cebon, **Teaching Engineering Materials: the CES EduPack**

Large Quantity of Steel Products in China

Annual steel production in 2011 is 696 million tons， about 45.5% of the World.

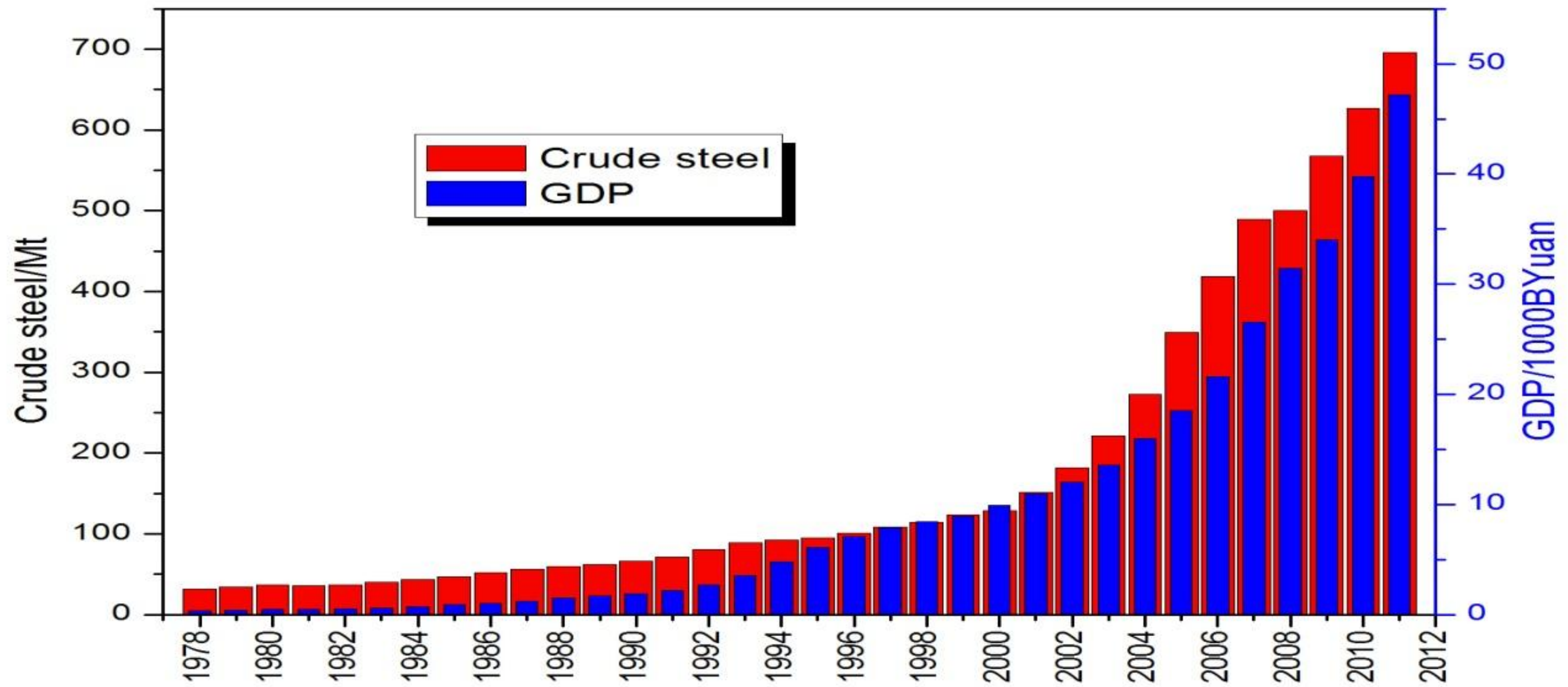

year	2000	2001	2001	2003	2004	2005	2006	2007	2008	2009	2010	2011
China	128	151	182	222	282	353	419	489	500	560	627	696
World	848	850	904	970	1069	1147	1251	1351	1327	1200	1414	1527
%	15.1	17.7	20.1	22.8	26.3	30.7	33.4	36.1	37.6	46.6	44.7	45.5

Large Quantity of Automobiles in China

Automobile annual sale in 2011 is 18.51 million, ranked No.1 in the world.

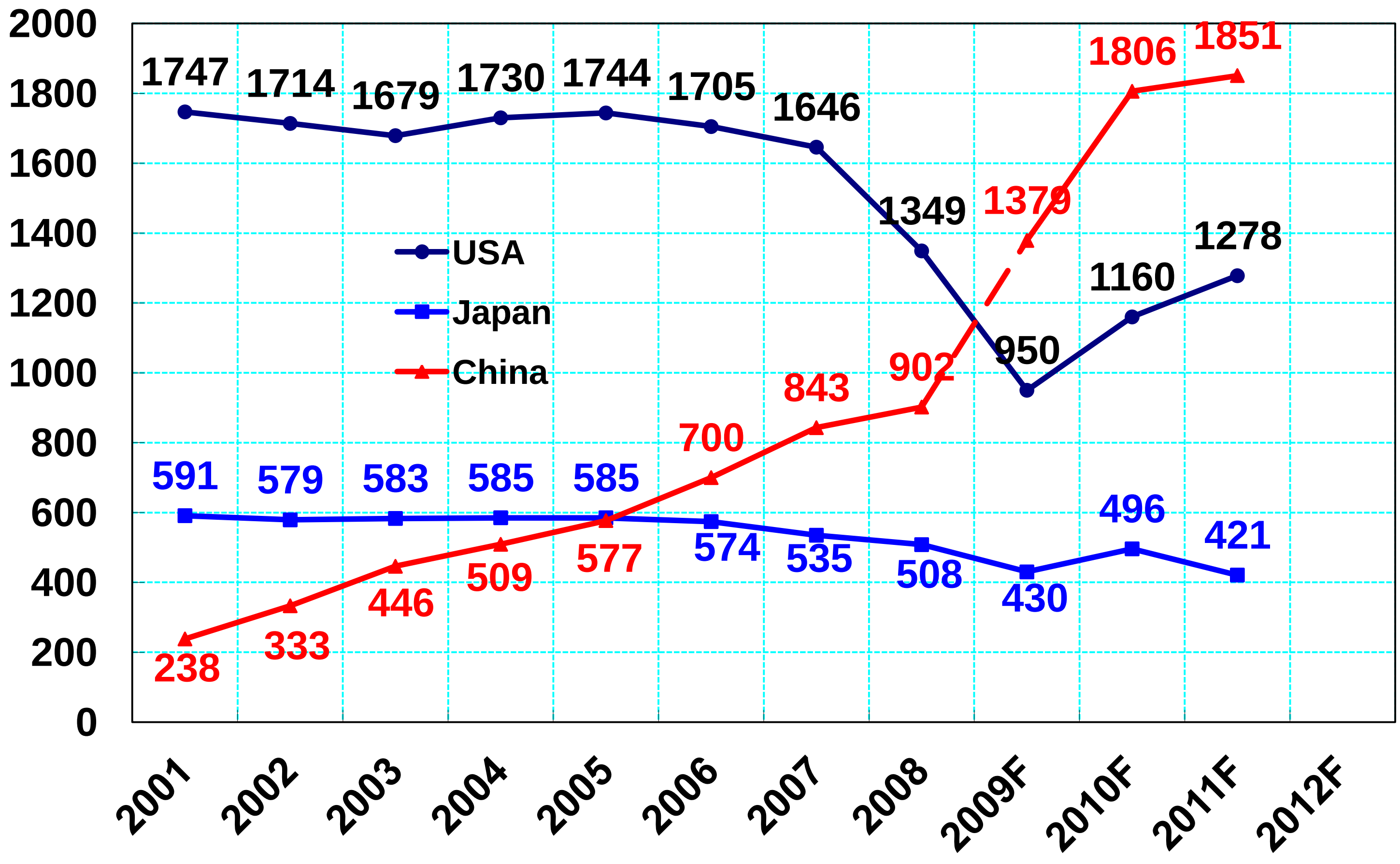

Automobile lightweight and Safety——
Strive to develop advanced high strength steel

Automobile lightweight is urgent measure under the pressure caused by environment and resource

➢～8% petrol saved if automobile weight reduced 10%*.

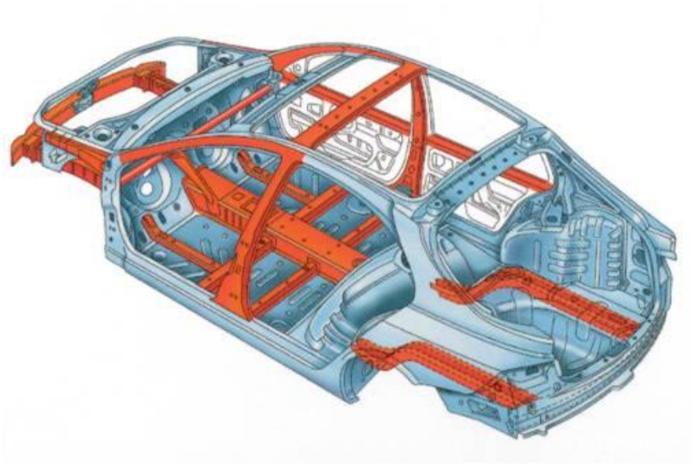

Advanced high strength steel is the first choice of automobile structure materials

	1975	2005	2007	2015	Change From 1975 to 2015
Mild Steel	2,180	1,751	1755	1,314	Down 866 lbs.
HSS and Bake Hard	140	324	327	325	Up 185 lbs.
Advanced / Ultra HSS	--	111**	149**	403**	Up 403 lbs.
Iron	585	290	284	244	Down 341 lbs.
Aluminum (includes castings)	84	307	327	369	Up 285 lbs.
Plastic/Composites	180	335	340	364	Up 184 lbs.

*: Takehide SENUMA, ISIJ International, 2001, 41, 520-532

*3rd generation AHSS

- UTS > 1000 MPa
- Elongation 20% or more
- Low cost（alloying elements、processing）

Feasible microstructure？

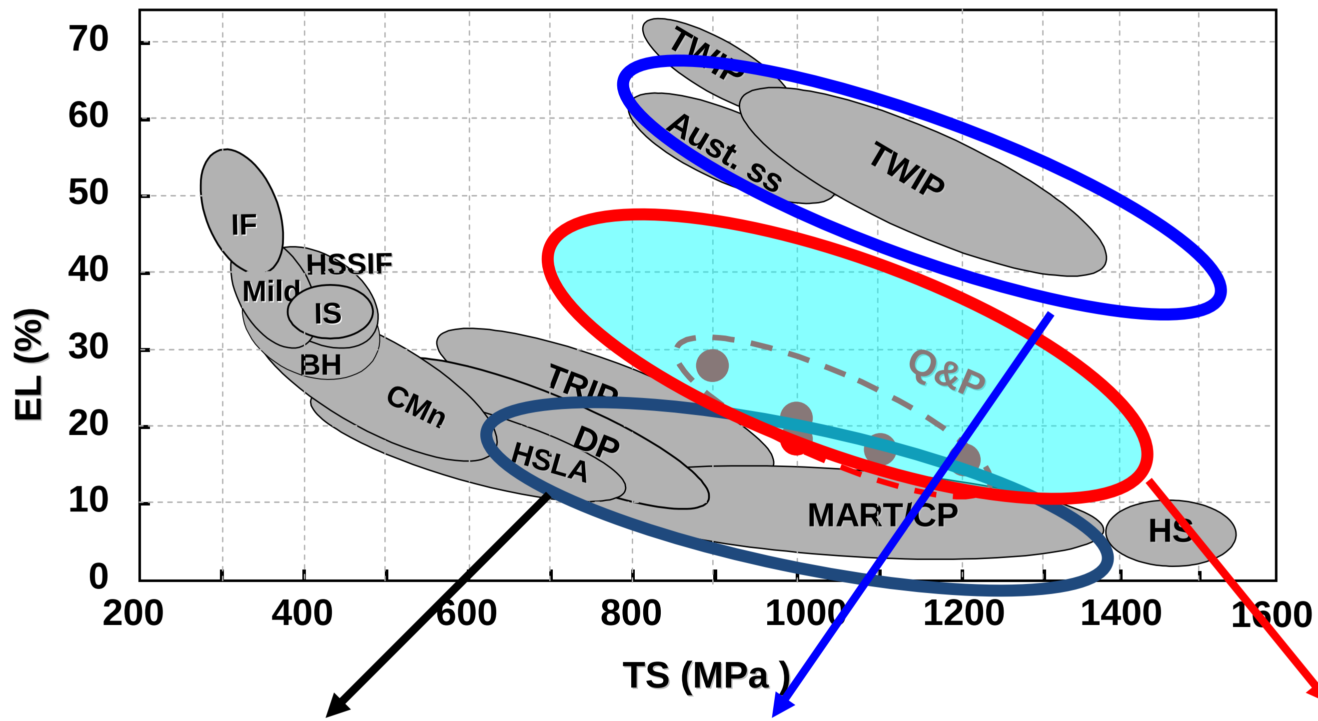

Challenge Opportunity

1st AHSS	2nd AHSS	3rd AHSS
<15000MPa·%	50000MPa·%	20000MPa·%

D. K. Matlock, J. G. Speer, The 3rd International Conference on Advanced Structural Steels, Gyeongju, Korea, August 22-24, 2006, 774.

3rd AHSS target microstructures

Matrix Strengthening TRIP Precipitates Strengthening

Hard(M)＋Soft(RA)＋Precipitates

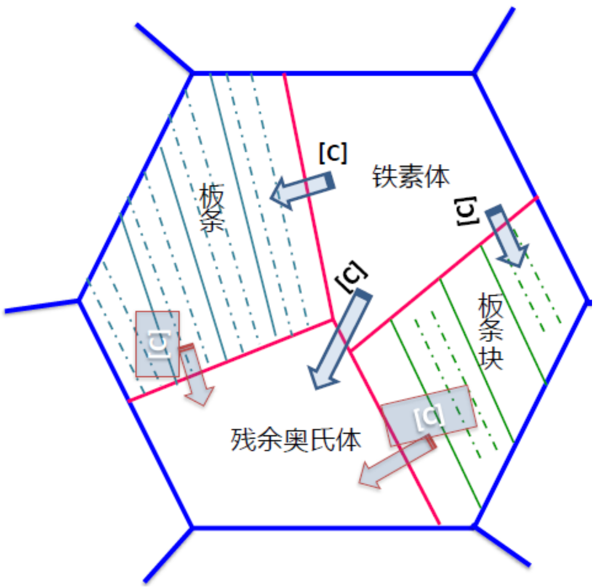

QP or QPT

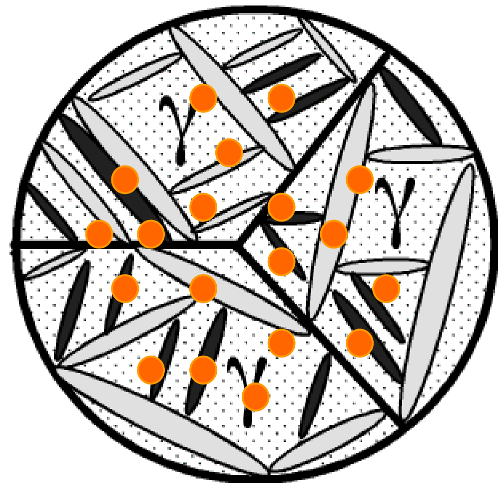

Lath martensite + retained austenite + nano scale precipitate

Microstructure control

Local VS Overall ！

Interface (Block & Packet)

Fraction / morphology / size etc. for Soft RA

Why lath martensite (~ 0.4 C%)?

- Complicated microstructure for lath martensite
  - prior austenite grain
  - packet (habit plane)
  - block (OR)
  - lath (low angle)
- Several possible strengthening mechanism
  - Substantial and interstitial solid ha
  - Dislocation strengthening, i.e. work
  - Fine twins
  - Grain size
  - segregation of carbon atoms
  - Precipitation of iron carbons

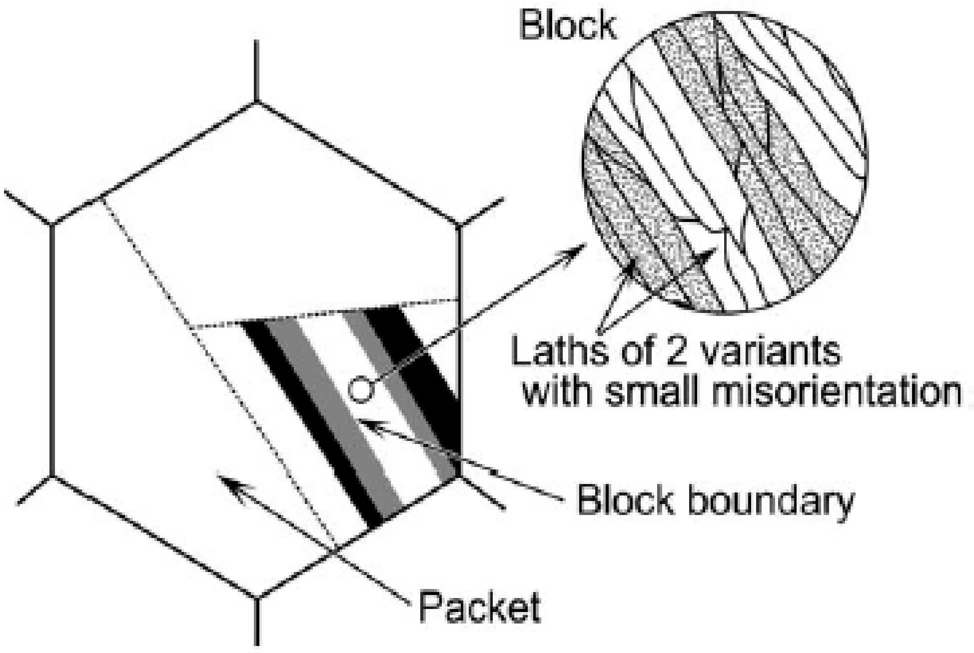

Morito S, et al. Acta Mater, 2003, 51: 1789

AHSS with high alloying elements (high cost)

Steels	Compositions										
	C	Ni	Cr	Mo	Co	Mn	Si	Ti	Al	S	P
AF 1410E	0.16	10.05	1.99	1.01	13.80	0.16	0.051	0.01	0.01	0.003	0.001
AerMet100	0.24	11.08	3.04	1.20	13.40	0.01	0.001	0.01	0.0099	0.001	0.003
4340	0.40	1.78	0.79	0.26		0.69	0.26		0.031	0.003	0.016

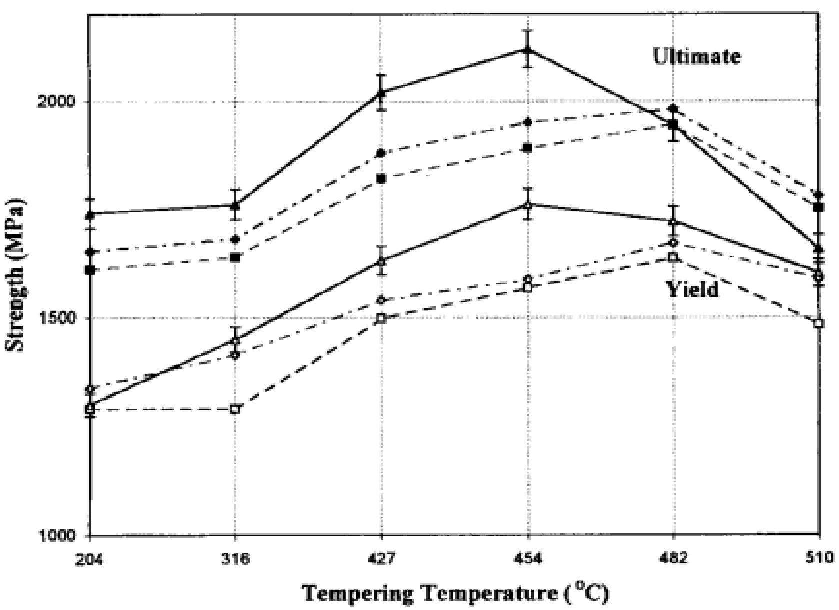

Variation of yield and ultimate strength as a function of tempering temperature.

Box: AF 1410 E + 1Cr; diamond: AF 1410E; and triangle: AerMet 100.

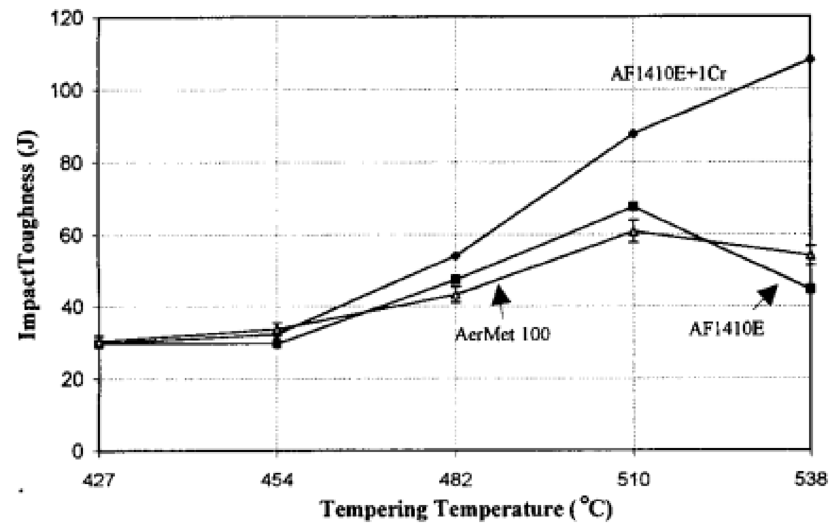

Effect of tempering on Charpy notch toughness of AF 1410E and AF 1410E + lCr steels

Maraging steels
Precipitation

Ayer R, Machmeire PM(1996) Microstructural basis for the effect of chromium on the strength and toughness of AF1410-based high performance steels. Metall Trans 27A: 2510-2517

Progress II： Steels with Enhanced Toughness

- 0.4C- 2Si-1Cr-1Mo

nano precipitation on suitable matrix

Processing	500-600° C tempering	500° C+1.7 (Strain Ageing)
UTS (MPa)	1770	1850
YS (MPa)	1470	1840
A (%)	10	15
VE (J)	14	**226**

Lath martensite
＋nano precipitate
= “bamboo”

A
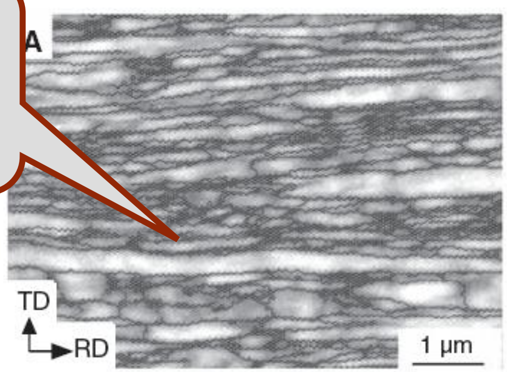

B
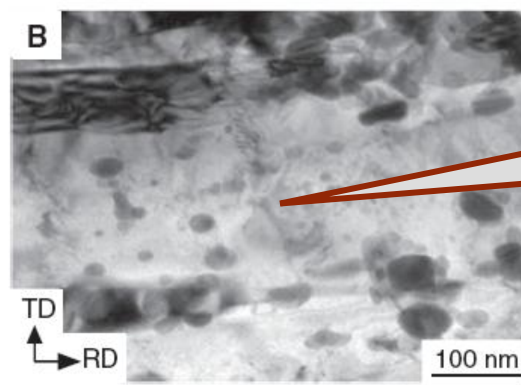

C

Dispersed nano precipitation

Yuuji Kimura, Tadanobu Inoue, Fuxing Yin, **Kaneaki Tsuzaki**， science， vol. 320， 2008

Progress III： Nano bainite steels

Nano scale microstructure

Nano ferrite＋nano austenite＝nano bainite

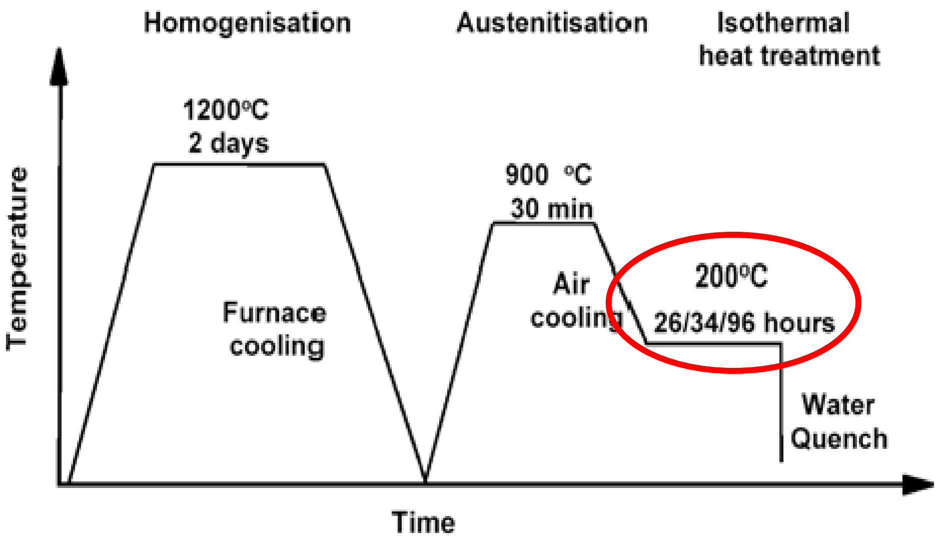

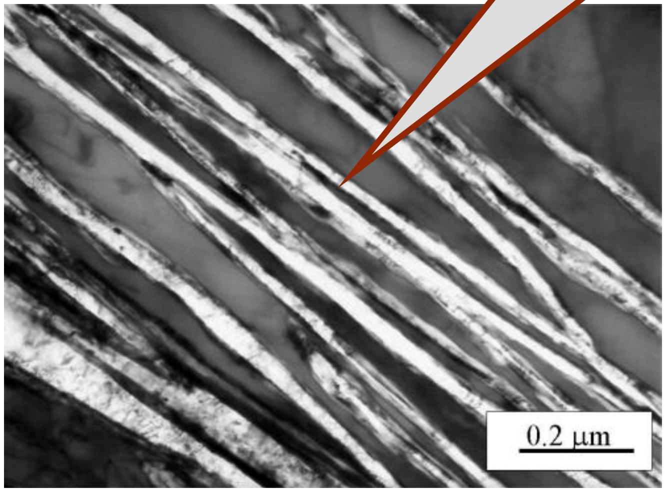

Steel	C	Si	Mn	Cr	Mo	V	Co	Al
A	0.79	1.59	1.94	1.33	0.30	0.11	–	–
B	0.98	1.46	1.89	1.26	0.26	0.09	–	–
C	0.83	1.57	1.98	1.02	0.24	–	1.54	–
D	0.78	1.49	1.95	0.97	0.24	–	1.60	0.99

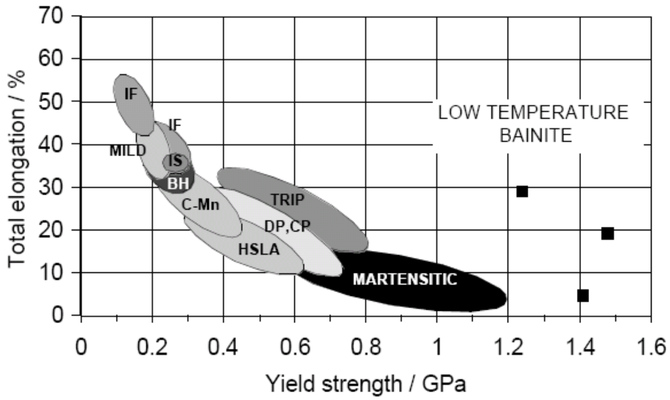

C. GARCIA-MATEO, F. G. CABALLERO and **H. K. D. H. BHADESHIA.** ISIJ International, Vol. 43 (2003), No. 8, pp. 1238–1243

Phase composition and grain size refinement

Steel type		Parameters	Phases
Single phase (Mild steel)	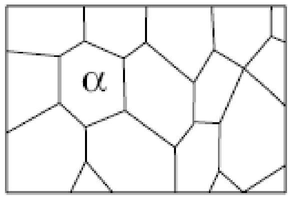	- Grain size - Grain shape	α = ferrite
Two phase (Dual phase steel)	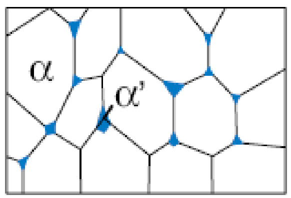	- Grain sizes - Volume fractions - Local chemical composition	α = ferrite α' = martensite
Multi phase (TRIP steel)	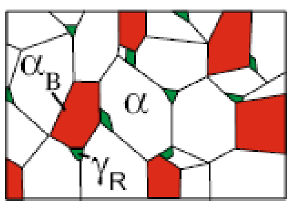	- Grain sizes - Volume fractions - Local chemical composition - Phase stability	α = ferrite α_B = bainite γ_R = retained austenite

Refinement

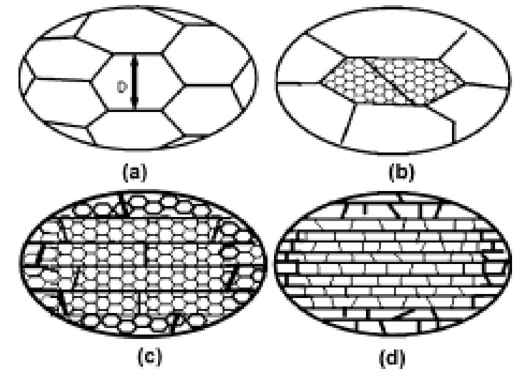

Local chemical composition & Phase stability !

Bleck, W. and K. Phiu-On, *Effects of Microalloying in Multi Phase Steels for Car Body Manufacture.* Microstructure and Texture in Steels, 2009: p. 145-163.

Suwas, S., A. Bhowmik, and S. Biswas, *Ultra-fine Grain Materials by Severe Plastic Deformation: Application to Steels.* Microstructure and Texture in Steels, 2009: p. 325-344.

Viewpoint: Routine for achievement of finer microstructure by combination of phase transformation and deformation in steels

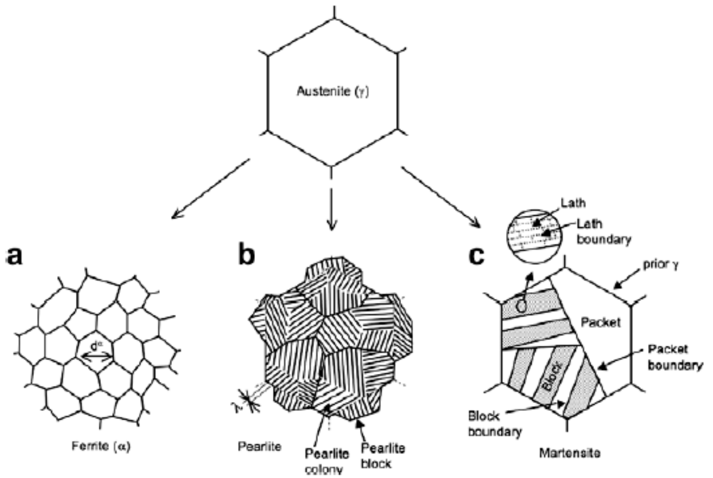

Figure 2. Three typical microstructures obtained by phase transformation in steels. (a) Ferrite structure. (b) Pearlite structure. (c) Martensite structure.

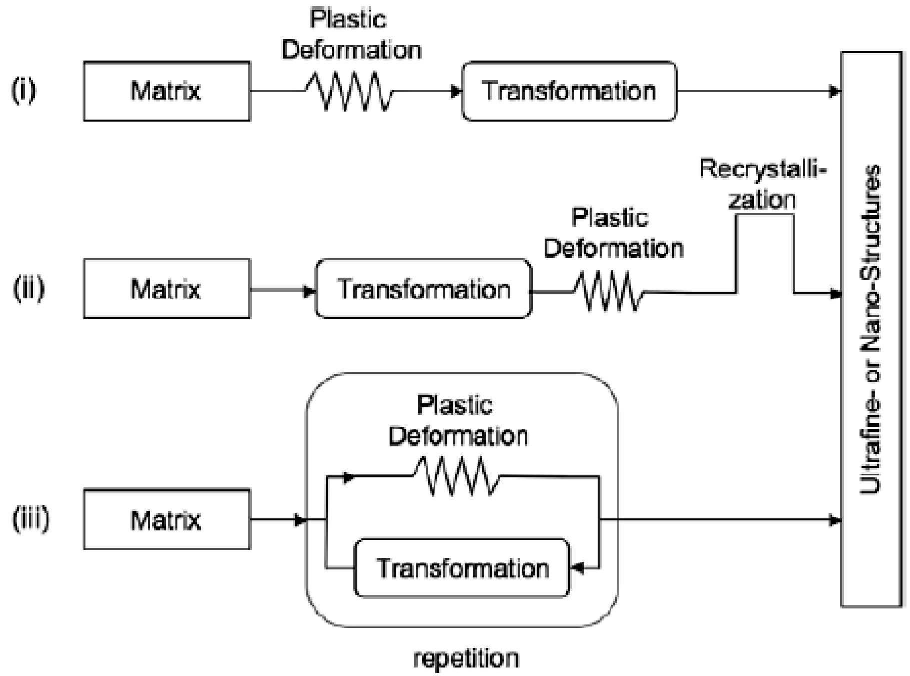

Figure 1. Three different sequences combining phase transformation and plastic deformation for the fabrication of nanostructured metals. (i) Plastic deformation of the mother phase prior to phase transformations. (ii) Plastic deformation after phase transformation. (iii) Repetition of plastic deformation and phase transformation.

N. Tsuji and T. Maki, Scripta Materialia 60 (2009) 1044–1049

Processing along with Alloying Effects for Fe-C Steels

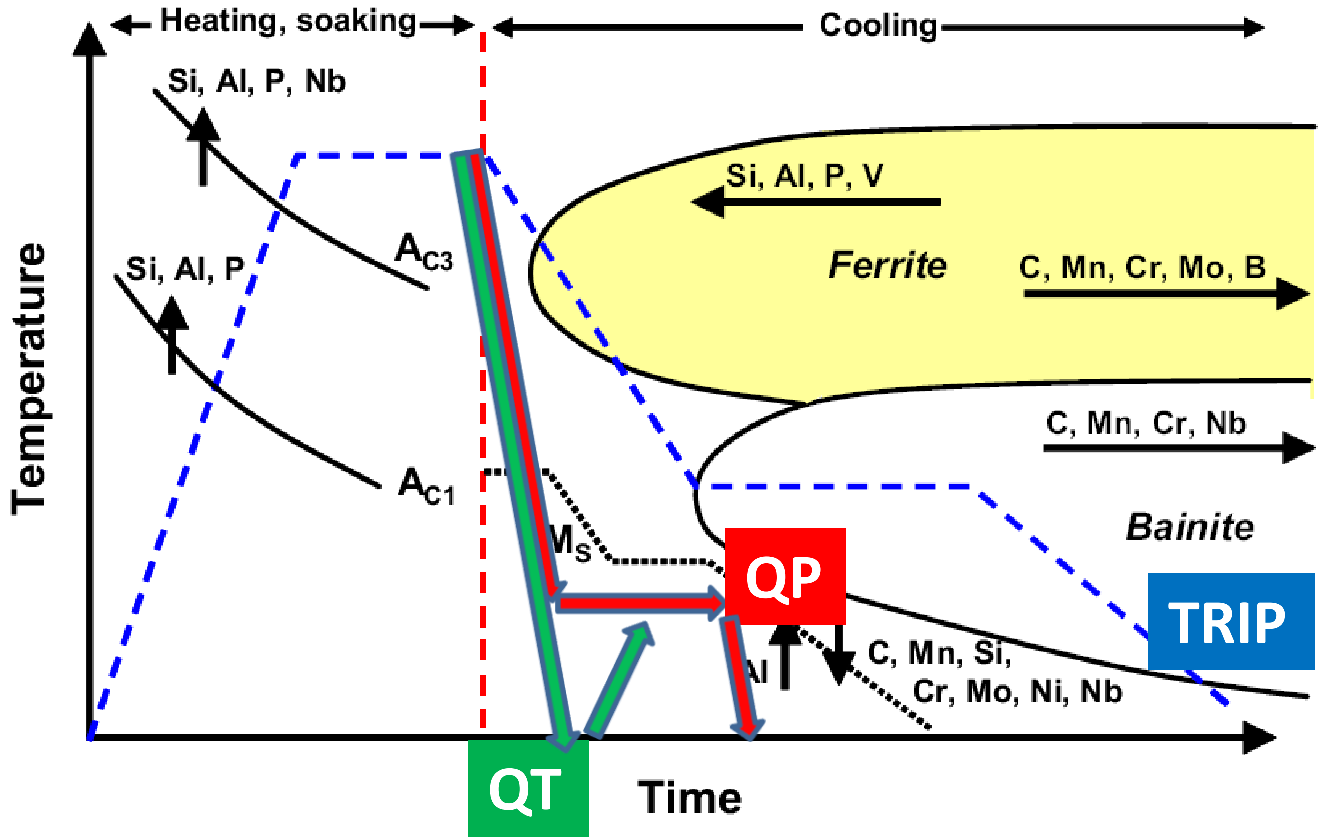

Microstructure of
Metastable Multi-scale Multi-phase

- Composition
- Processing

Bleck, W. and K. Phiu-On, *Effects of Microalloying in Multi Phase Steels for Car Body Manufacture.* Microstructure and Texture in Steels, 2009: p. 145-163.

Suwas, S., A. Bhowmik, and S. Biswas, *Ultra-fine Grain Materials by Severe Plastic Deformation: Application to Steels.* Microstructure and Texture in Steels, 2009: p. 325-344.

OUTLINE

- Introduction
- **Quenching and Partitioning Treatment**
  - Processing and Alloying
  - Microstructure and properties
  - Competing Process and Kinetics Models
    - Carbide formation and suppression
    - Migration of the martensite/austenite interface
    - Carbon partitioning and partitioning kinetics
- Combination of QPT with Hot Stamping and Application Concerns
- Unresolved Issues
- Concluding remarks

* Schematic Process for QP & QPT

Quenching: Fraction of Martensite
Partioning: Carbon diffuse into residual austenite

C-Si-Mn

15000MPa·%

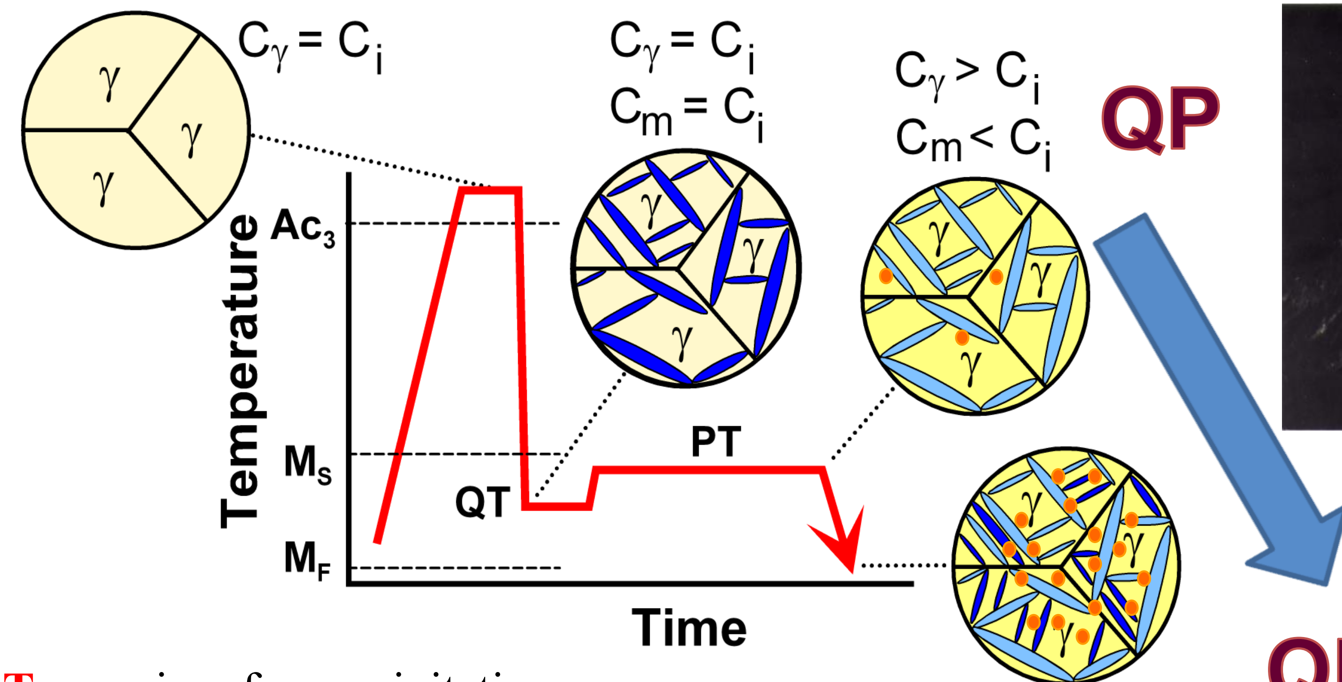

Tempering: for precipitation

Speer&Edmonds, 2003, QP
T. Y. Hsu, 2007, QPT

Microalloying + tempering = strengthening by precipitatoin

> 15000MPa·%

T. Y. Hsu (Xu Zuyao)， Materials Science Forum (2007)

1) Composition of steels feasible for QPT Treatment

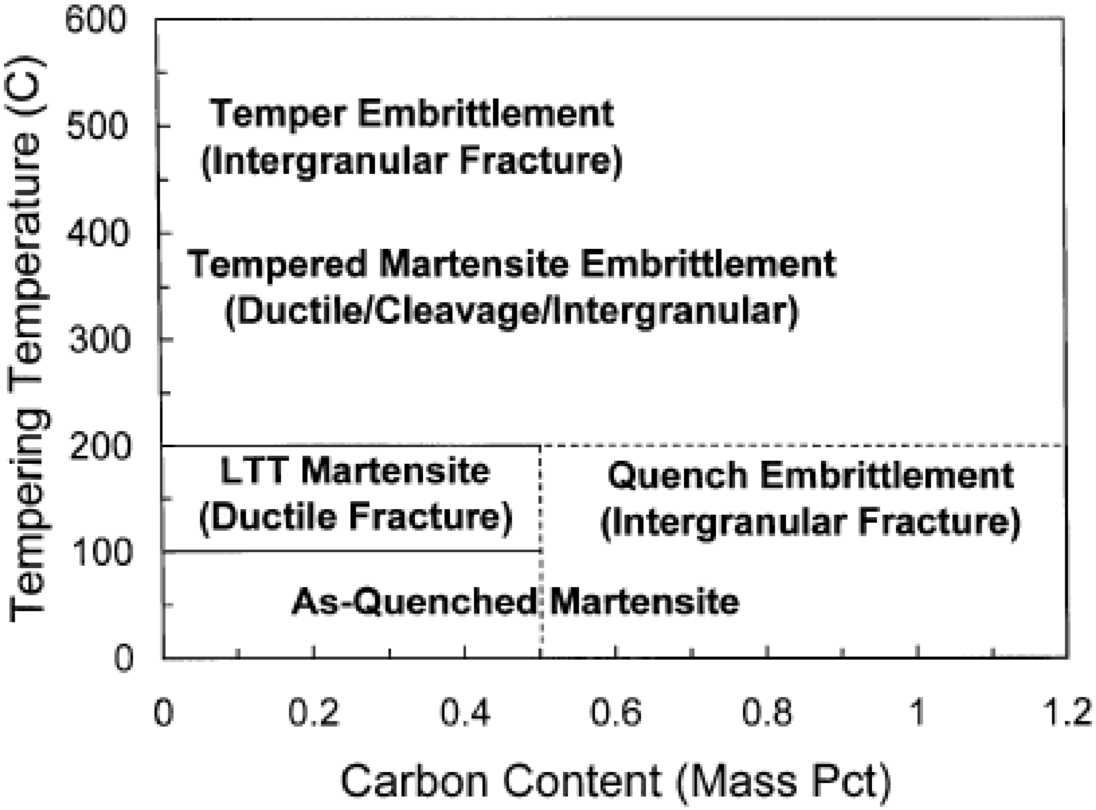

Although high carbon content is beneficial for strengthening, embrittlement is along with it, therefore, **low carbon (<0.5wt%) is necessary**.

Krauss revealed that >0.5% of carbon content in carbon and low alloyed steels would lead quench and temper embrittlement resulted from **cementite formation**

(G. Krauss. Metall. Trans., 2001, 32B: 205-221.)

Designed chemical compositions：

as <0.5C, 1.5Si(or Al), 1.5Mn with(or without) 0.2Mo and 0.02Nb(mass%).

fine lath martensite; dispersed complex or ε(η) carbide precipitated in martensite and retained austenite with certain carbon content, and considerable thickness as well as fine grain size of original austenite.

First try for a TRIP with high Si by J Speer et al

Steel	C	Mn	Si	P	Al
Low Si	0.15	1.5	0.3	0.005	0.03
High Si	0.15	1.5	1.6	0.005	0.03
Al	0.15	1.5	0.1	0.005	1.9
P	0.15	1.5	0.3	0.1	0.03

% γ, before isothermal transformation at lower hase lower-carbon austenite. Microstructures Figure 5. At 300°C the microstructure is lath the holding time increased, the lath features in (b) and (c), presumably a result of an etching response to the tempering. There is no bainite formation at this temperature, in contrast to the behavior discussed above for the intercritically annealed condition. While retained austenite is usually not expected in 0.15 wt.% C martensite, a small amount was detected by x-ray diffraction, possibly indicating some carbon partitioning between the martensite and austenite prior to final cooling to room temperature.

J.G. Speer, D.K. Matlock, B.C. De Cooman, and J.G. Schroth:
Acta Mater., 2003, vol. 51, pp. 2611–22.

158 44^{th} MWSP Conference Proceedings, Vol. XL, 2002

96200	Weight %
C	0.56-0.64
Mn	0.75-1.00
P	0.035 (max)
S	0.04 (max)
Si	1.80-2.20

1700 MPa @ 8 % for QT at 425C

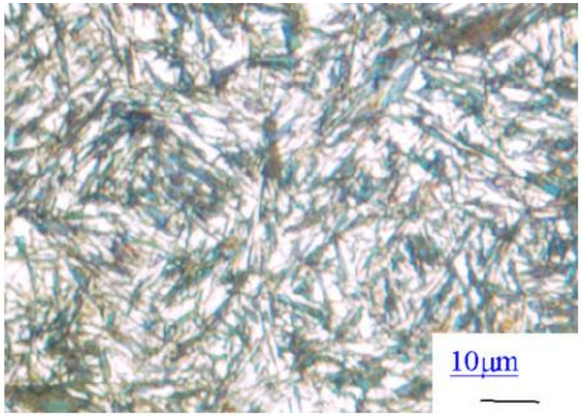

Fig. 6—Light optical micrograph of Q&P microstructure in AISI 9260 steel quenched to 463 K (190 °C) and partitioned at 673 K (400 °C).[36] Nital etch; retained austenite appears white.

F.L.H. Gerdemann, J.G. Speer, and D.K. Matlock: Proc. Materials Science and Technology 2004, TMS/AIST, Warrendale, PA, 2004, pp. 439–49.

4) Evidence for carbon partitioning

TABLE I. Activation energies in kilojoule per mole associated with the observed exothermic DSC peaks.

	Peak 1	Peak 2
Q&P 350 °C 10 s	92	172
WQ		170

TABLE II. Reported activation energies in kilojoule per mole for tempering stages, bainite formation, and element diffusion.

		E (kJ/mol)	Ref.
Tempering stages	C clustering	67–91	15
		81–94	7
	ε/η formation	102–135	7
		111–118	7
		127	19
	γ_{ret} decomposition	174	14
		202	19
	Cementite formation	233	19
		227	14
Bainite formation		45	21
		49	22
		43	23
Diffusion in bcc Fe	Fe pipe diffusion	152	20
	C	84	18

0.20C-1.63Mn-1.63Si

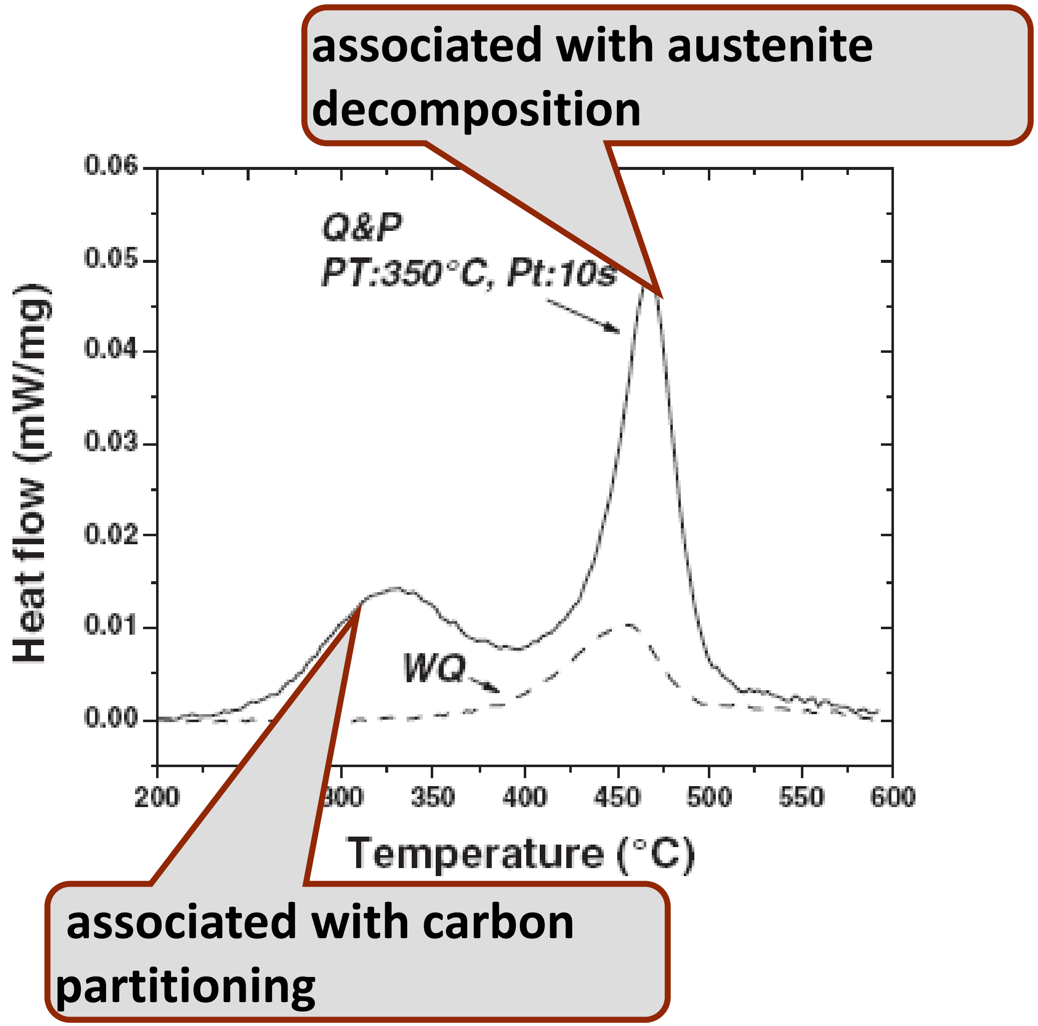

DSC heat flow as a function of temperature obtained after heating the CMnSi Q&P steel

Emmanuel De Moor， et al. PHYSICAL REVIEW B **82**, 104210 2010

Case 2) Quenching Tempering VS Quenching Partitioning

- **0.41C-1.27Si-1.30Mn-1.01Ni-0.56Cr**

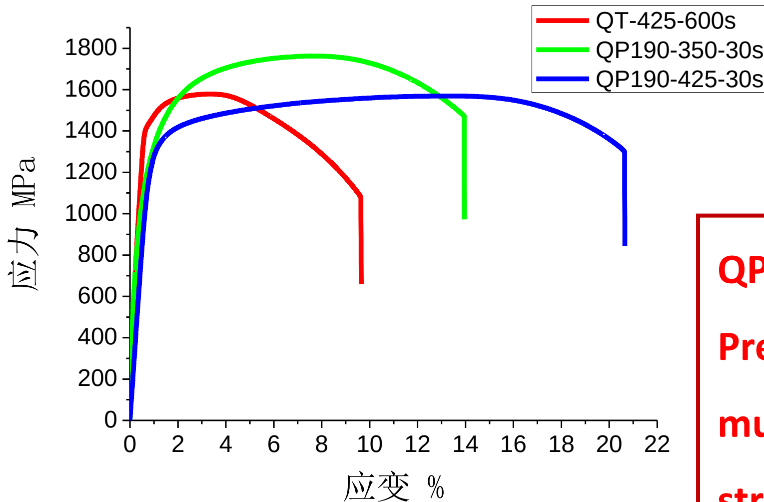

QPT2:

Precise control of multi-scale structure

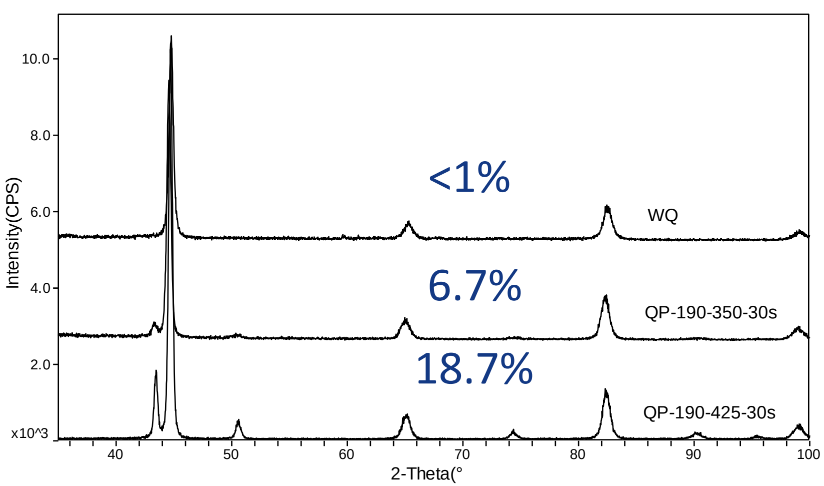

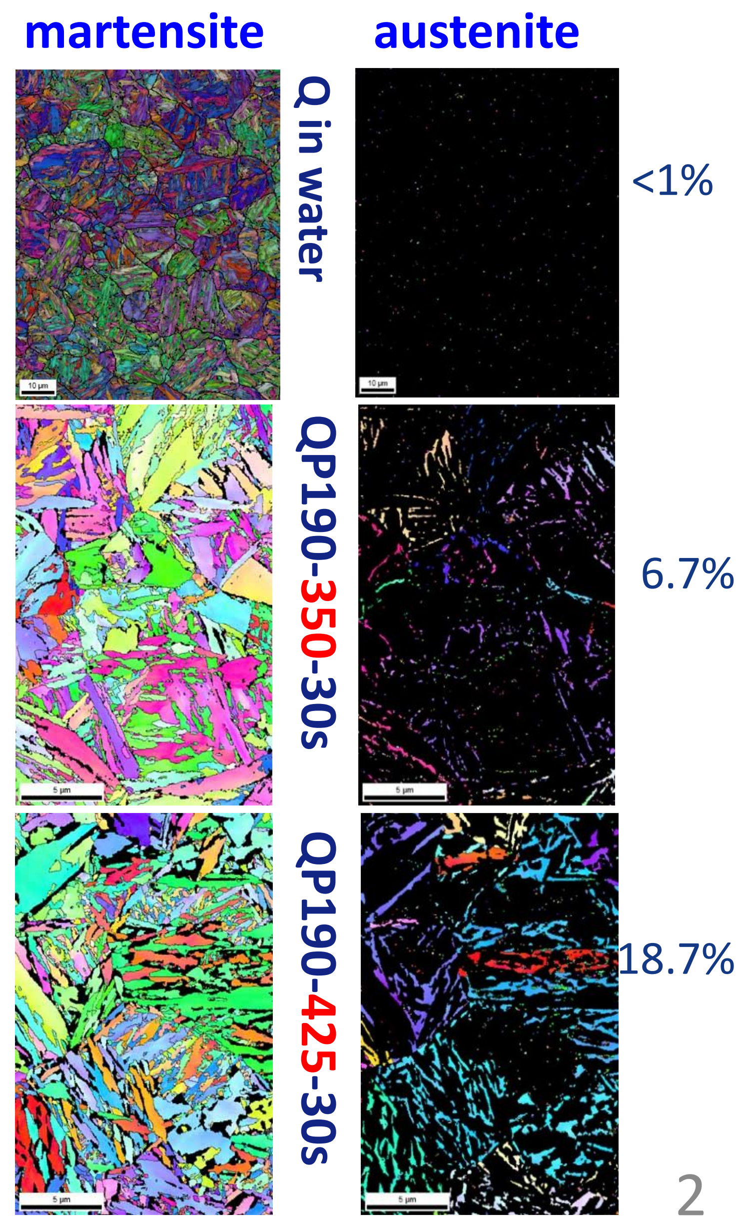

Y. H. Rong, et al, Acta Mater Sinica 2011

3) Epsilon precipitating during one-step QPT

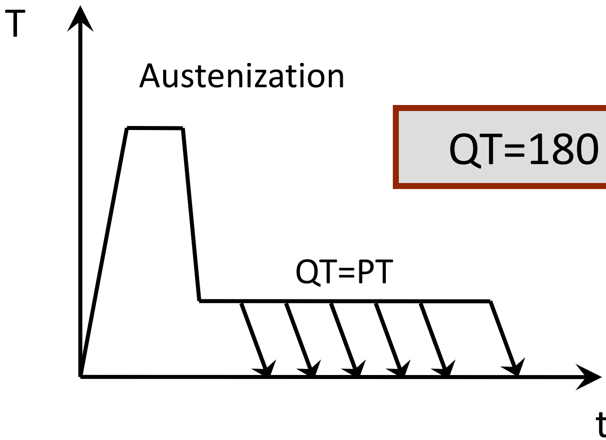

QT=180° C

Table 1 Chemical compositions of the steel in this study (wt.%)

Steel	C	Si	Mn	Ni	Cr	M_s (℃)
	0.41	1.27	1.30	1.01	0.56	277

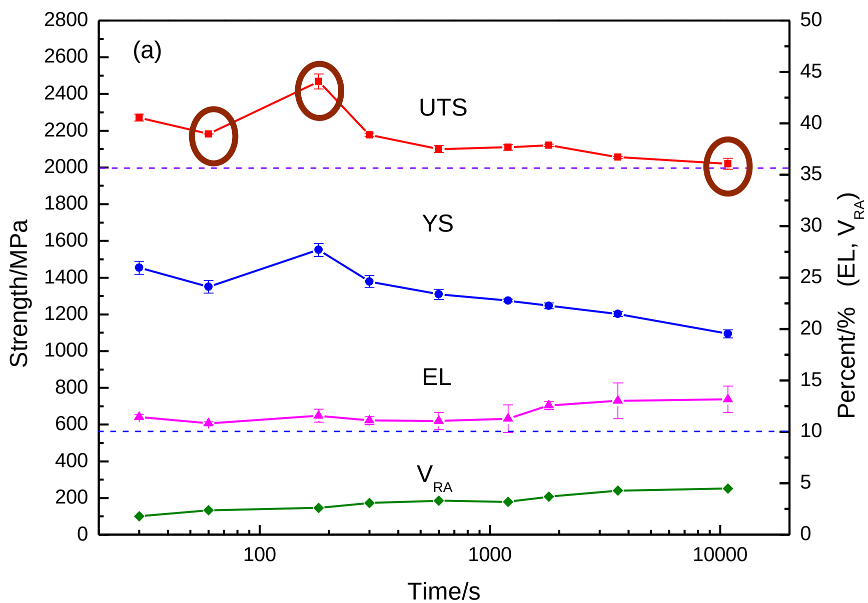

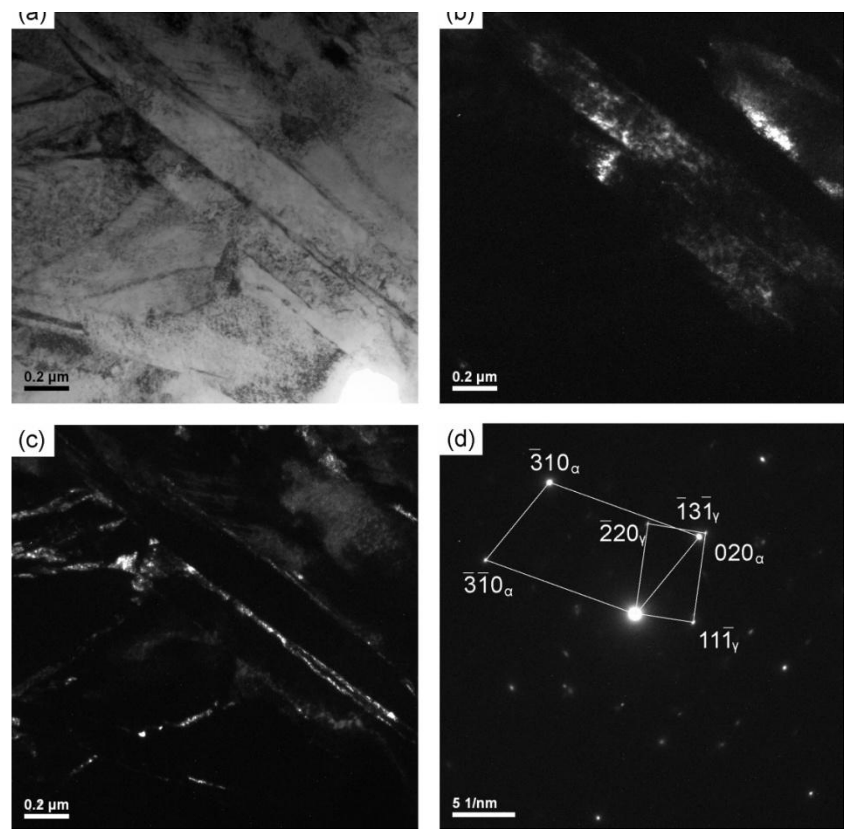

Typical TEM observations of Q&P steel quenched and partitioned at 180℃ for 30 s

H. Y. Li, X. W. Lu, W. J. Li, **X. J. Jin**, "Microstructure and Mechanical Properties of an Ultrahigh Strength 40SiMnNCr Steel during One-step Quenching and Partitioning Process", ***Metall and Mater Trans A***, **41** (2010) 1284-1300.

QPT treatment for a medium carbon steel

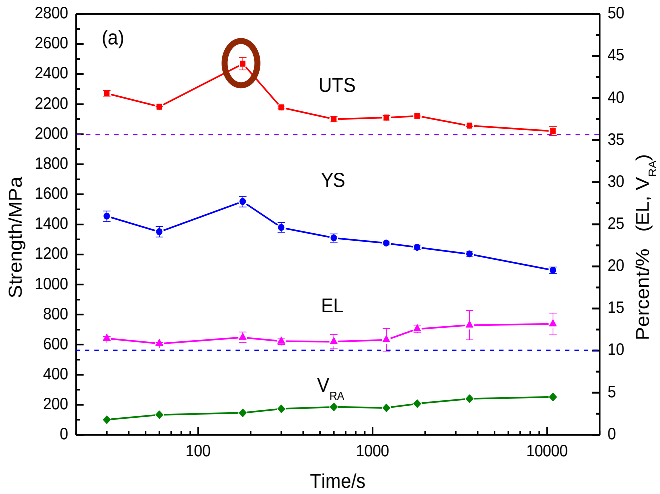

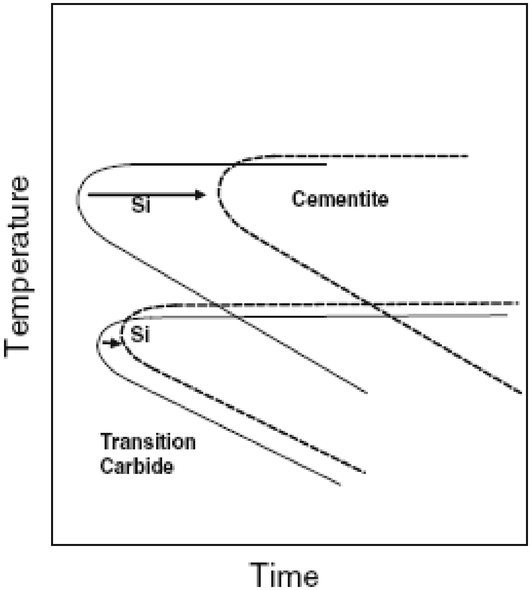

(c)

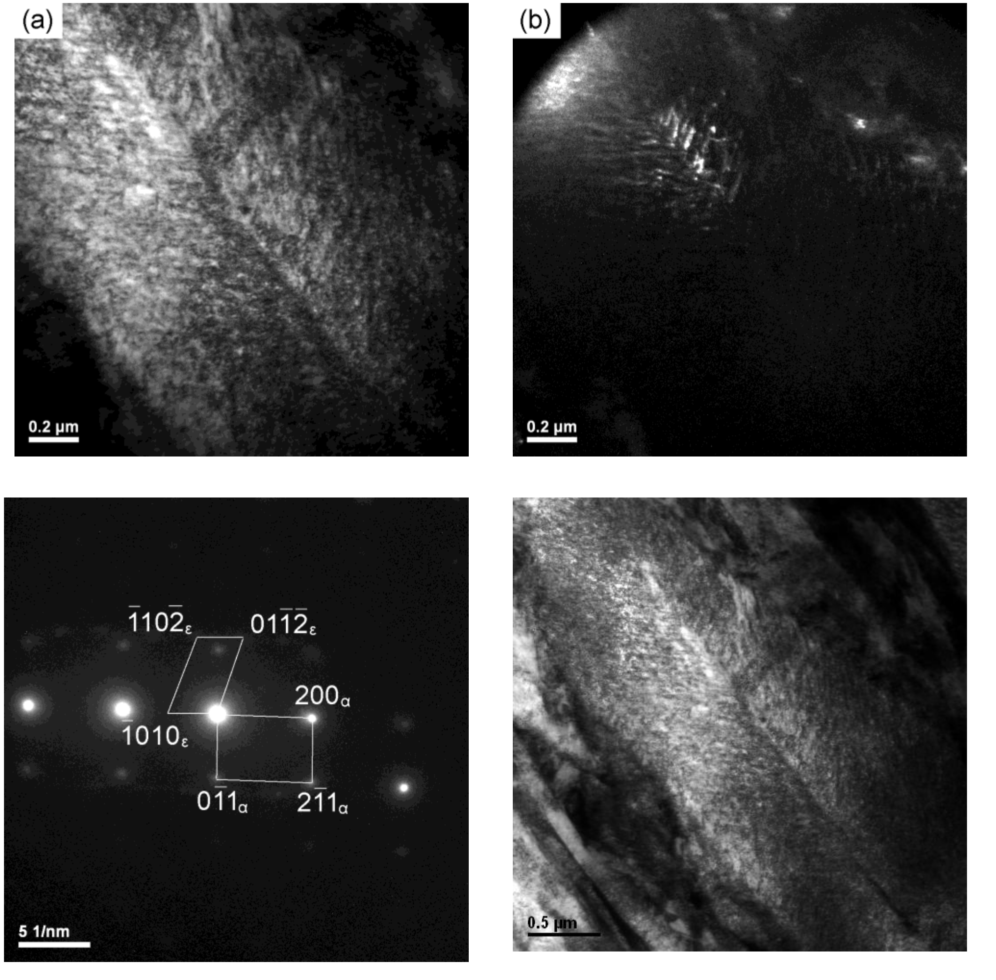

Transition carbide precipitation in the midrib of plate martensite during quenching and partitioning at 180℃ for 180s

D.V. Edmonds, K. He, F.C. Rizzo, B.C. De Cooman, D.K. Matlock, and J.G. Speer: Mater. Sci. Eng. A, 2006, vols. A438–440, pp. 25–34.

4) Low bainite transformation during QPT treatment

- **0.41C-1.27Si-1.30Mn-1.01Ni-0.56Cr**

Interior maintained at low level of carbon enable the bainite transformation during partitioning and tempering

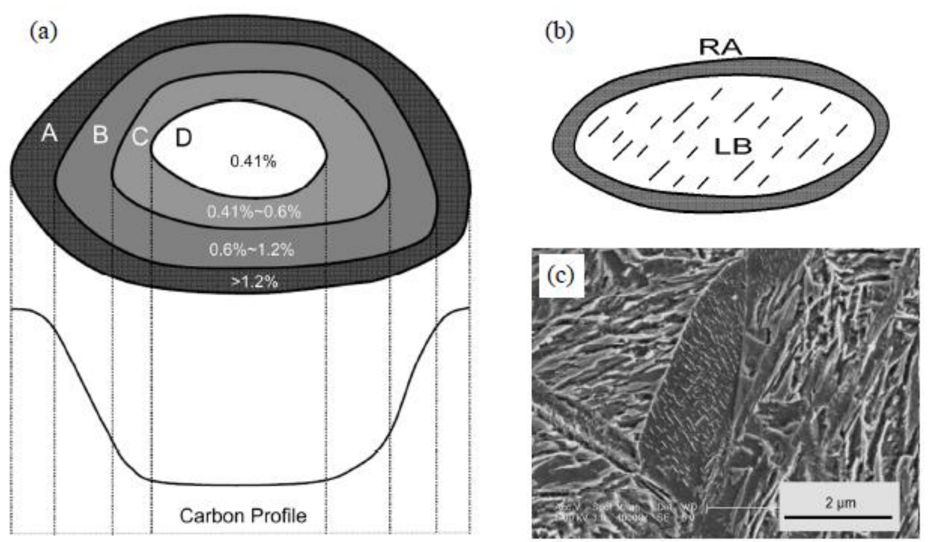

图 4.12 (a) 300°C 配分过程中未转变奥氏体池中碳浓度分布示意图; (b) 室温下残余奥氏体与

氏体形成的“橄榄状”组织示意图; (c) “橄榄状”组织的 FESEM 观察

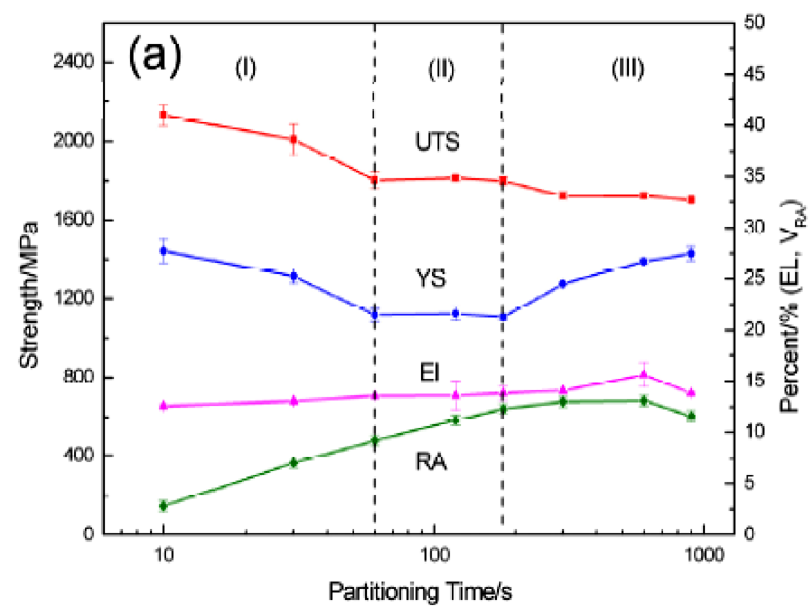

F. L. H. Gerdemann, J. Speer, G,, D. K. Matlock, in: MS&T2004 Conference Proceedings, New Orleans, 2004, pp. 439-43

H.Y. Li, X.W. Lu, X.C Wu, Y.A. Min, **X.J. Jin.** *Mater Sci Eng A（2010）*

Strengthening by Precipitation

TRIP 600

Fe-0.2C-1.53Si-1.46Mn

Fe-0.2C-1.5Mn-1.5Si-0.05Nb-0.13Mo

QT=220 C and PT=400 C (Ms=370 C)

1500MPa & 15%

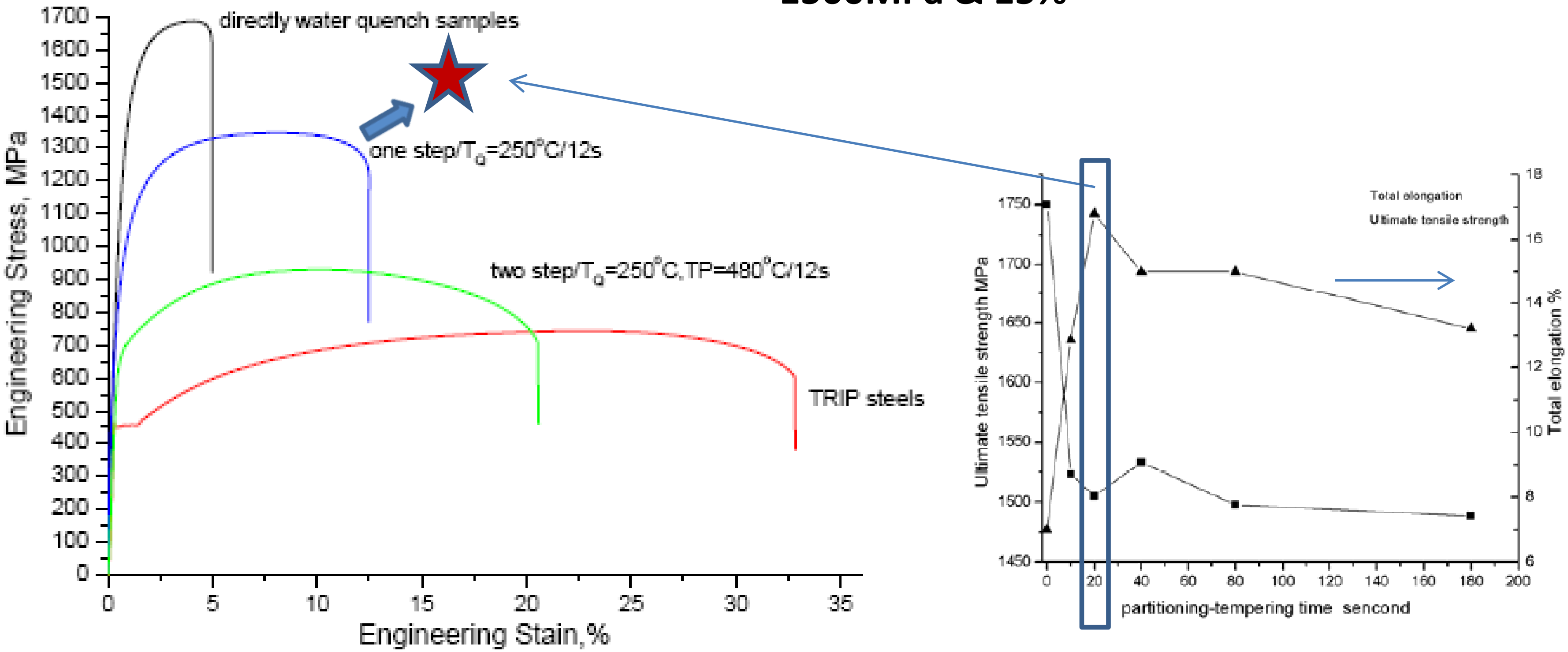

N Zhong, thesis, SJTU, 2009

Microstructure and properties for a medium carbon steel subjected to QPT

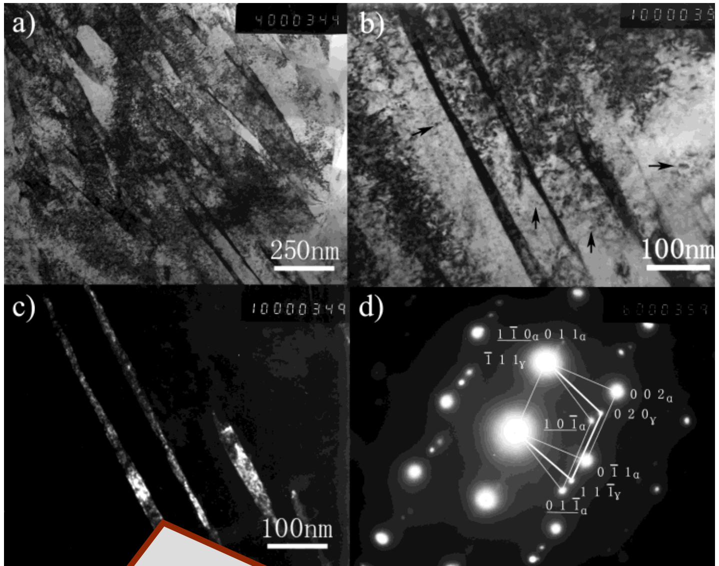

Martensite and austenite in nano scale

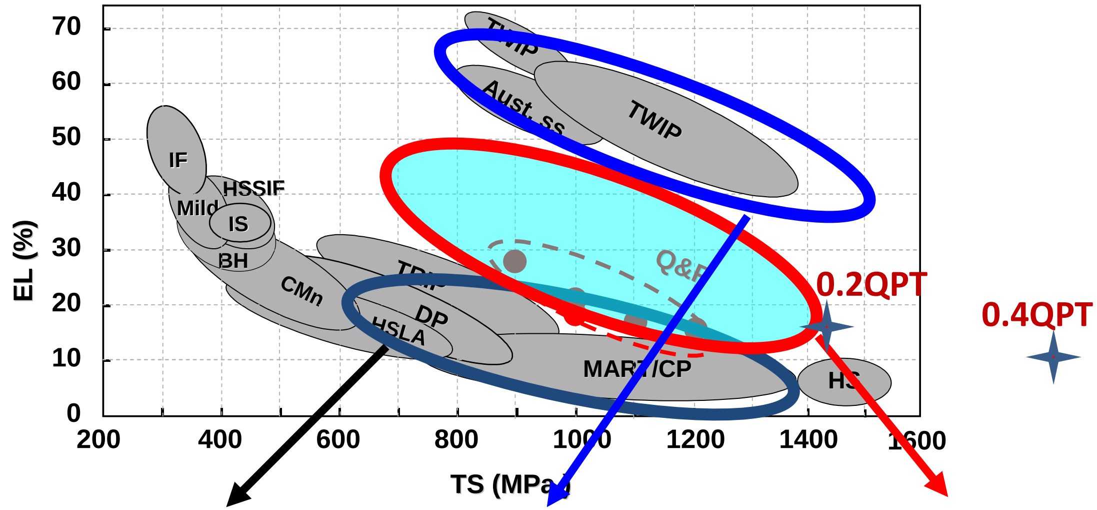

1st AHSS <15000MPa·%

2nd AHSS 50000MPa·%

3rd AHSS

20000MPa·%
Low alloying elements
Low cost of processing

Nano precipitates

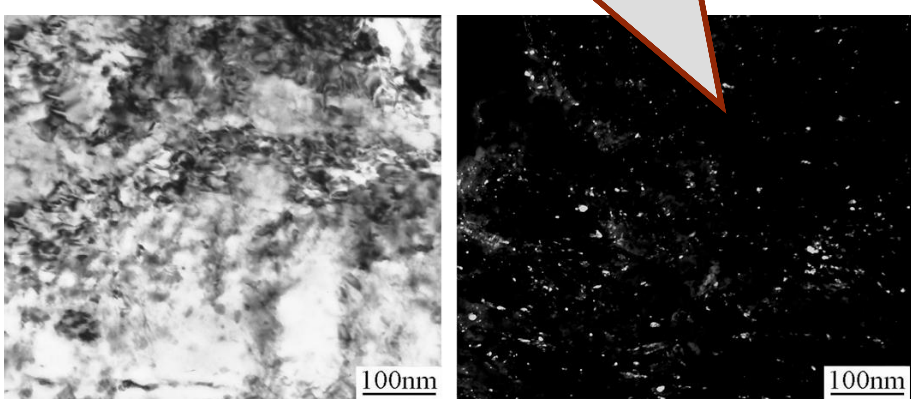

Fe-0.2C-1.5Mn-1.5Si-0.05Nb-0.13Mo
> 1500MPa & 15%

X. D. Wang, et al, J. Mater. Res 24 (2009) 261-267.

Multiphase Multiscale Metstable microstructure

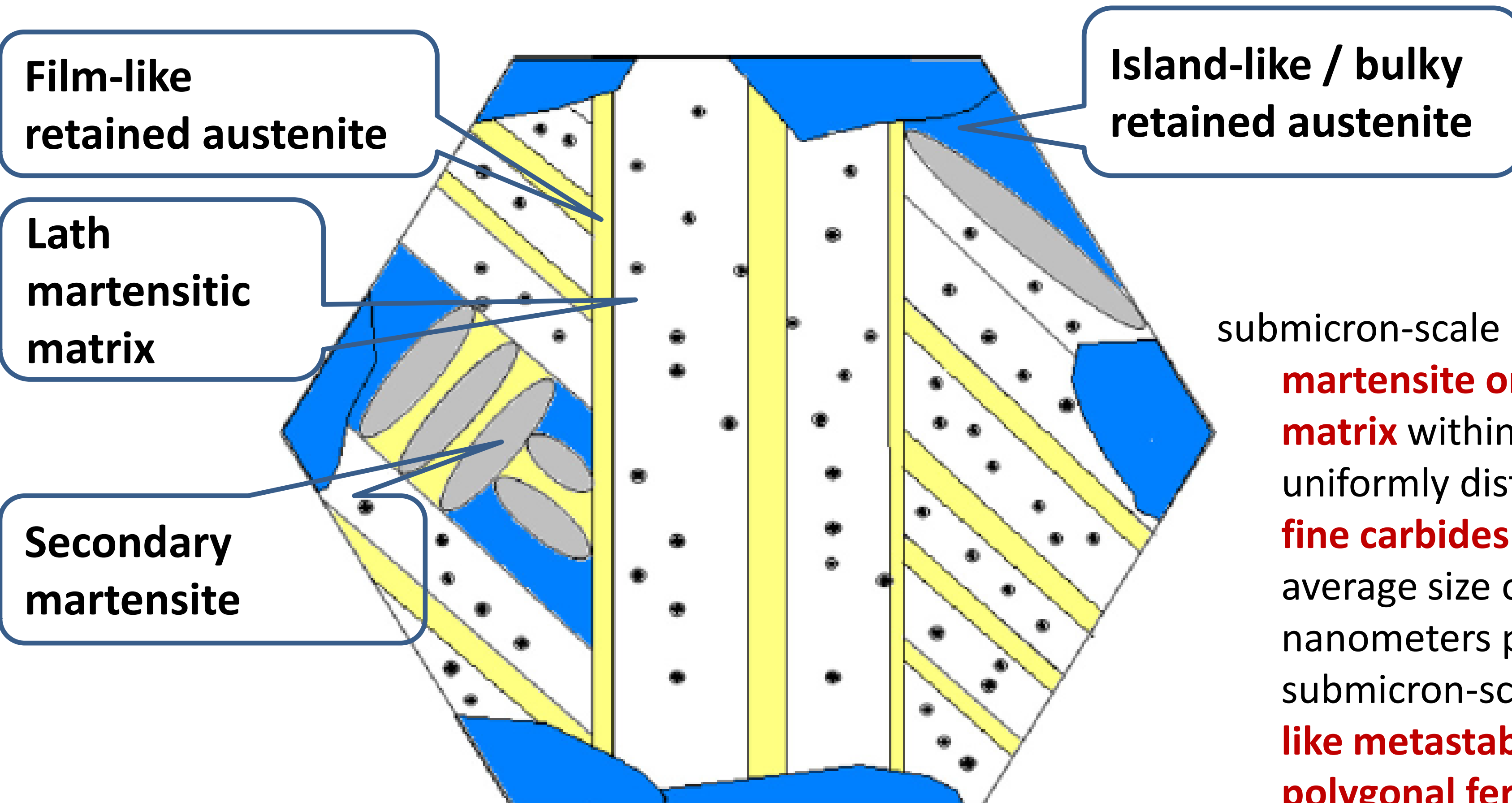

submicron-scale **lath martensite or bainite matrix** within which uniformly distributed **fine carbides** with average size of several nanometers plus submicron-scale **island-like metastable RA or polygonal ferrite** and **film-like RA** with film width of dozens of nanometers.

X. D. Wang, et al, Materials Science and Engineering A 529 (2011) 35– 40

Discussion
Third Generation AHSS property band

Tensile specimen geometry is well known to influence the measured value of total ductility.

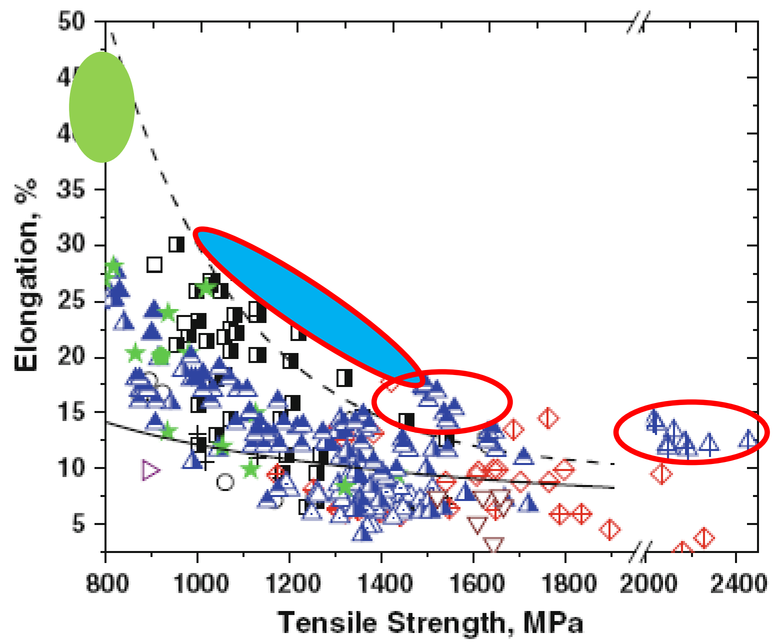

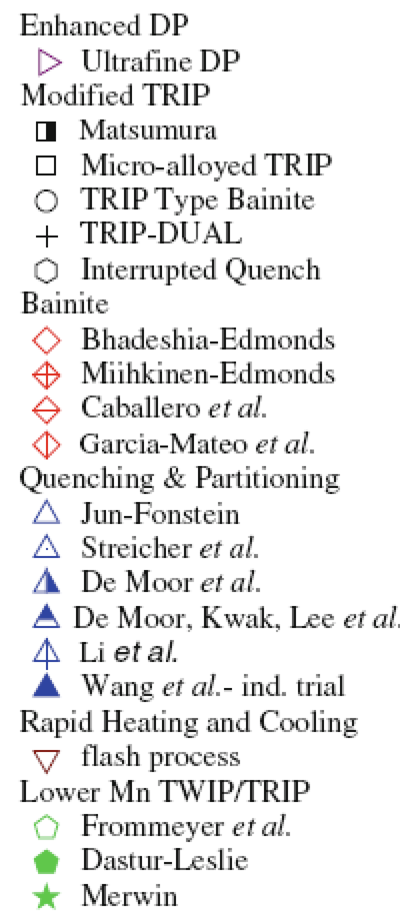

E. De Moor, P.J. Gibbs, J.G. Speer, D.K. Matlock, and J.G. Schroth: AIST Trans., 2010, vol. 7 (3), pp. 133–44.
J.G. Speer, D.K. Matlock , et al, METALLURGICAL AND MATERIALS TRANSACTIONS A, September 2011

OUTLINE

- Introduction
- Quenching and Partitioning Treatment
  - Processing and Alloying
  - Microstructure and properties
  - Competing Process and Kinetics Models
    - Carbide formation and suppression
    - Migration of the martensite/austenite interface
    - Carbon partitioning and partitioning kinetics
- **Combination of QPT with Hot Stamping and Application Concerns**
- Unresolved Issues
- Concluding remarks

Combination with Hot Stamping

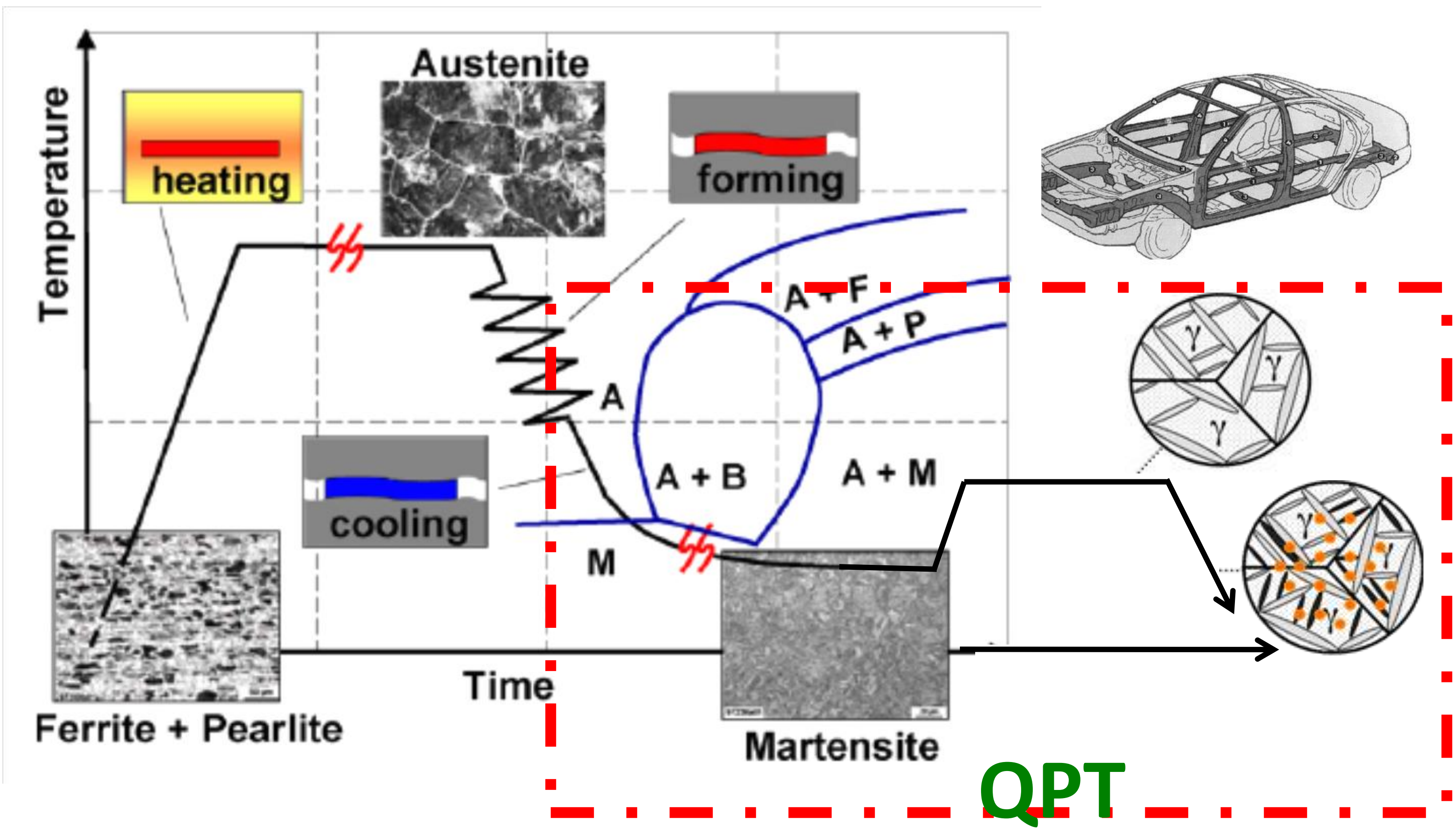

Control of microstructure through carbon partitioning !

1500 MPa
6 % elongation

?

Chemical compositions (wt. %) of both steels

steel	steel	C	Mn	Si	Ti	B	Al	P	S	Ms	Mf	Ae3
B	22MnB5	0.22	1.58	0.81	0.022	0.0024	-	0.0064	0.0014	378℃	265℃	800℃

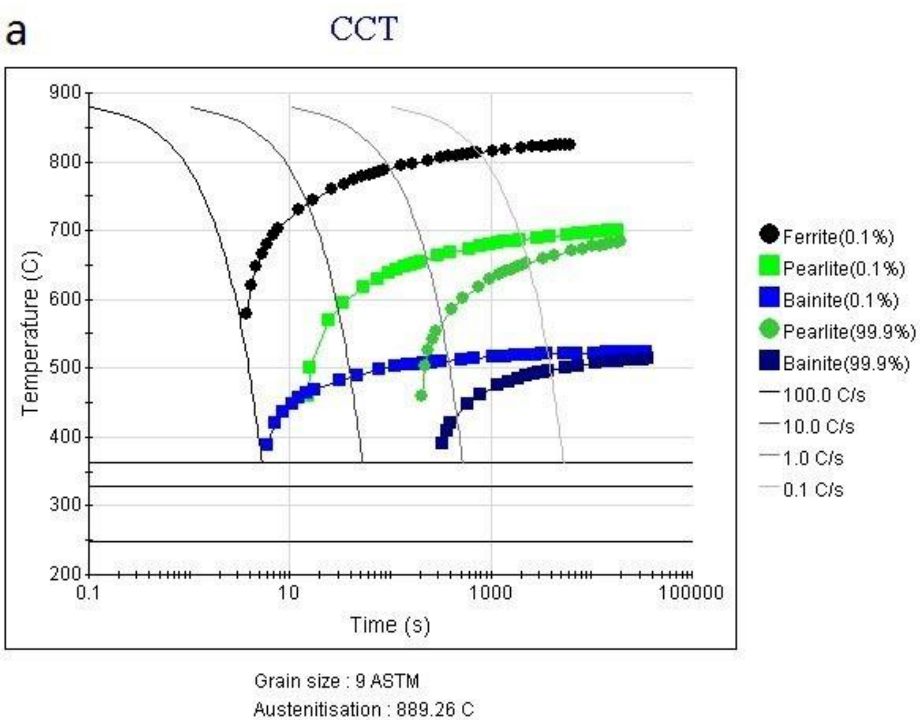

Steel A

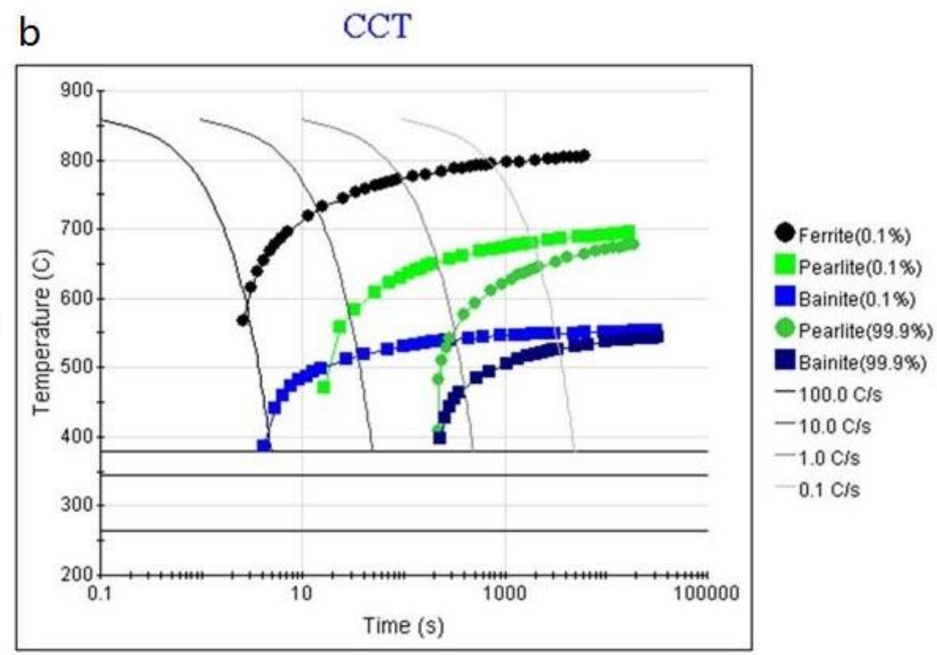

Steel B

Processing and specimen geometry

22SiMn2TiB steel with Ms=378°C and Mf=265°C

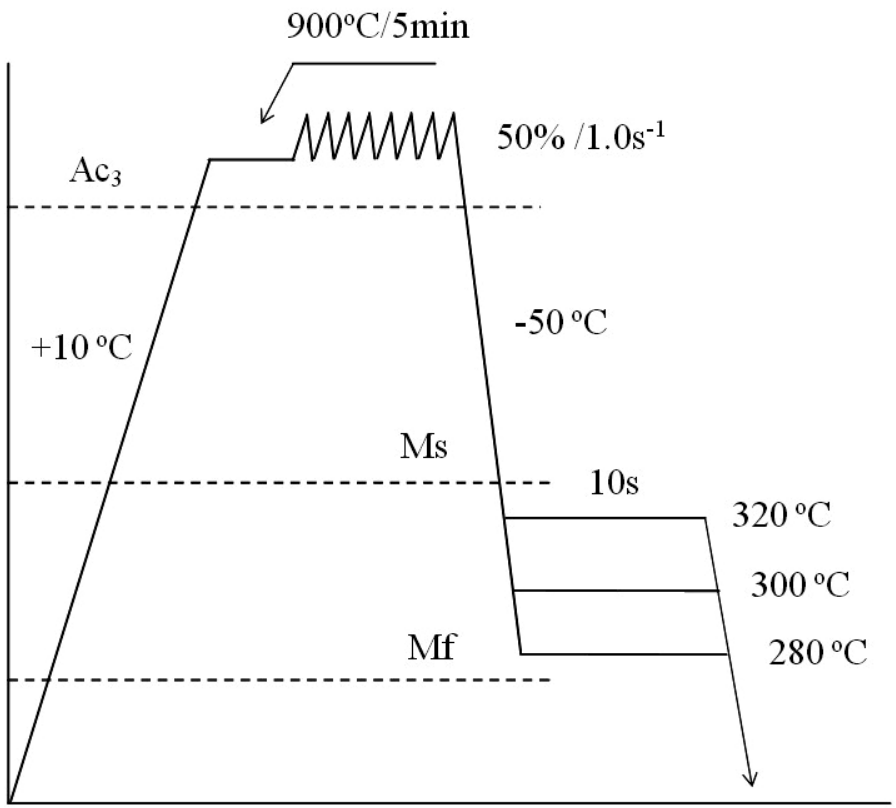

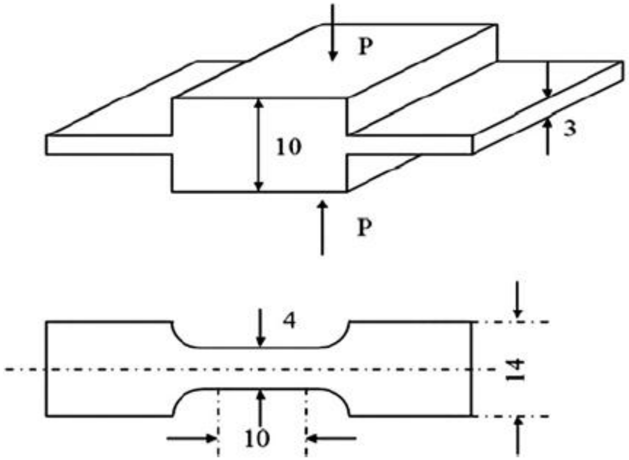

Preliminary results: Mechanical properties for specimens by combination of hot stamping and QPT

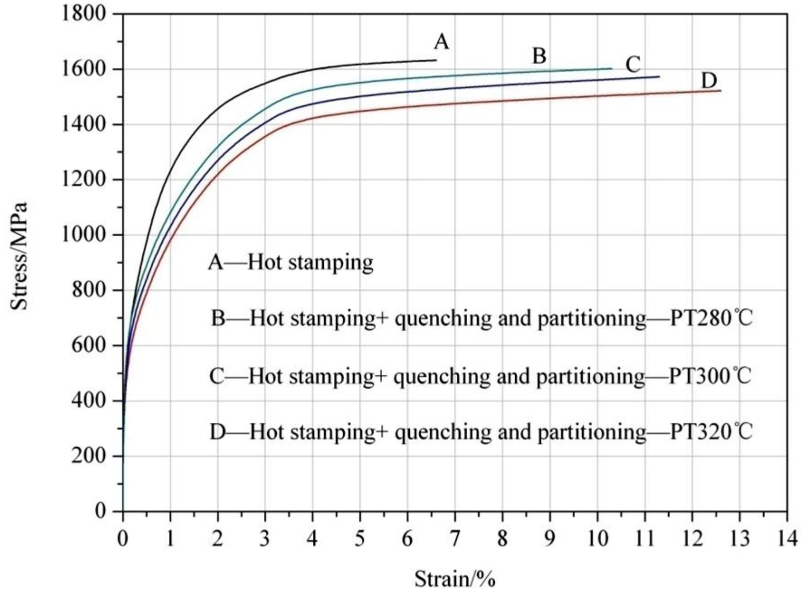

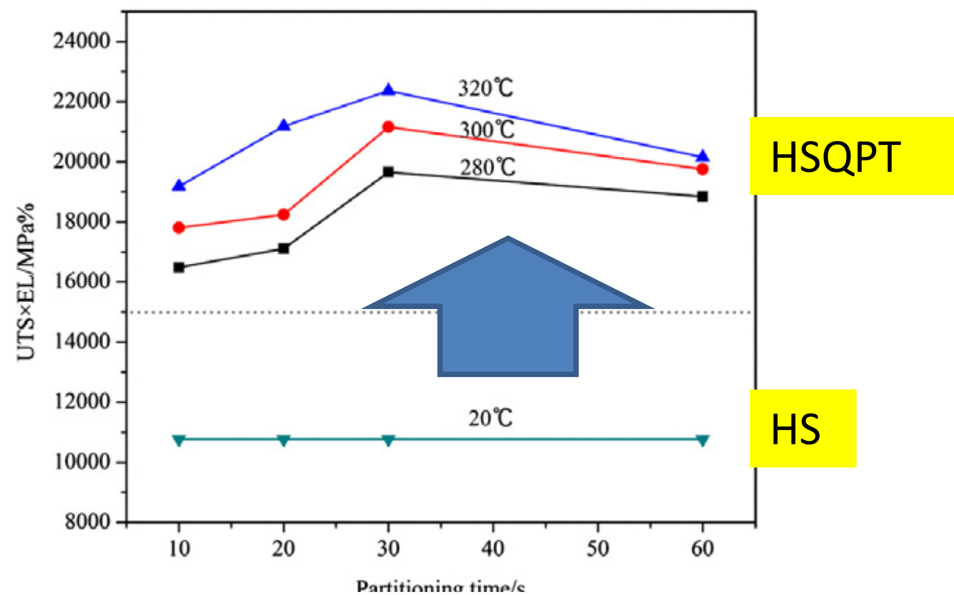

Table 1. The mechanical properties and amount of retained austenite after quenching at different temperatures.

Quenching temperature (°C)	Partitioning time (s)	Volume fraction of retained austenite (%)	Ultimate tensile strength (MPa)	Yield strength ($\sigma_{0.2}$) (MPa)	Elongation (%)
RT		<1	1632 ± 4	850 ± 3	6.6 ± 0.5
280	10	5.0 ± 0.5	1601 ± 5	720 ± 3	10.3 ± 1
300	10	10.1 ± 0.	1576 ± 5	696 ± 3	11.3 ± 1
320	10	15.6 ± 1	1522 ± 5	665 ± 3	12.6 ± 1
	20	17.3 ± 1	1569 ± 5	660 ± 3	13.5 ± 1
	30	18.5 ± 1	1510 ± 5	655 ± 3	14.8 ± 1
	60	16.6 ± 1	1562 ± 5	658 ± 3	12.9 ± 1

H. P. Liu and X. J. Jin* et al, ***Scripta Mater 64*** (2011) 749-752.

Finer Microstructure

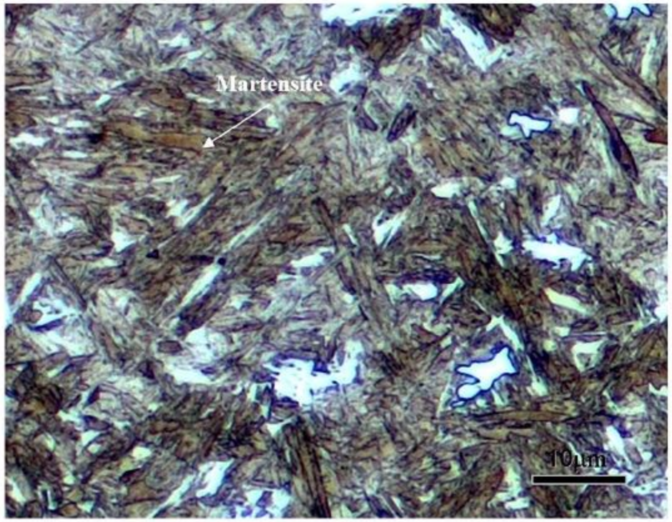

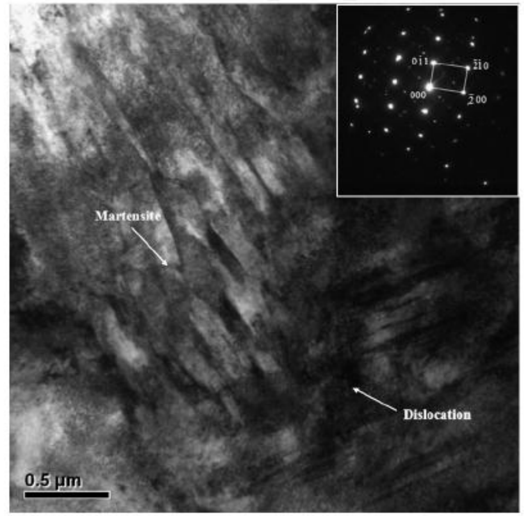

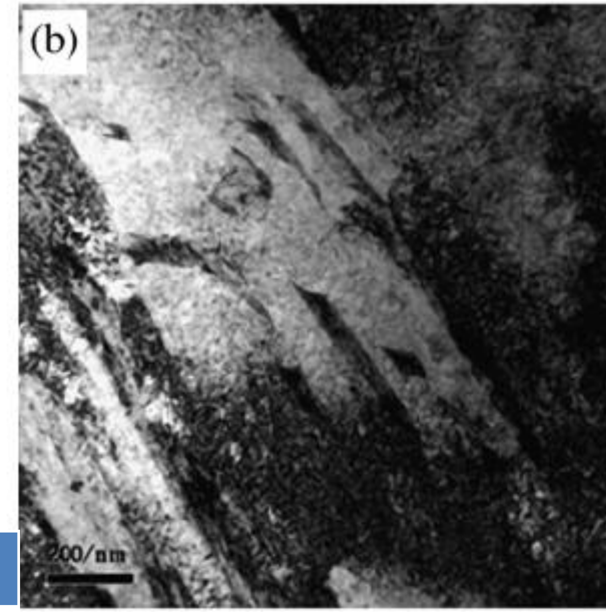

Optical image	**TEM for martensite**	**Austenite in BF**
Schematic representation of microstructure		Austenite in DF

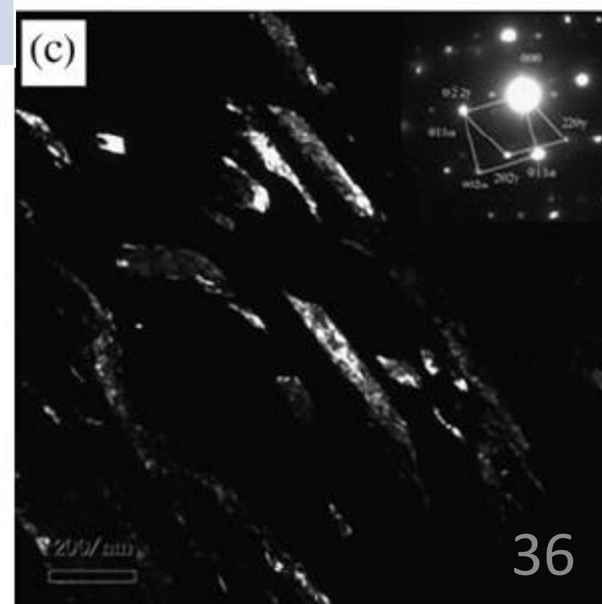

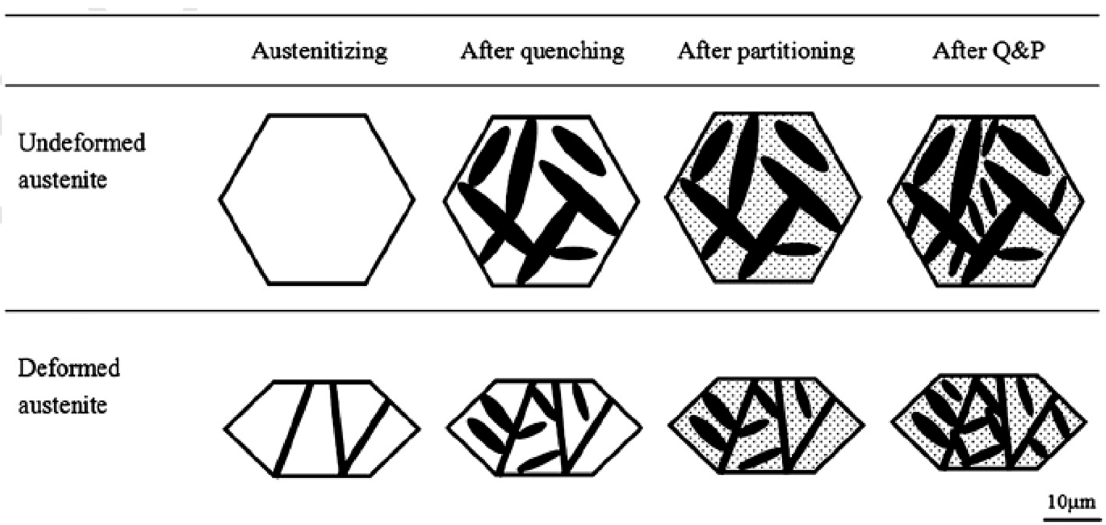

Preliminary result of laser welding

- **0.41C-1.27Si-1.30Mn-1.01Ni-0.56Cr**

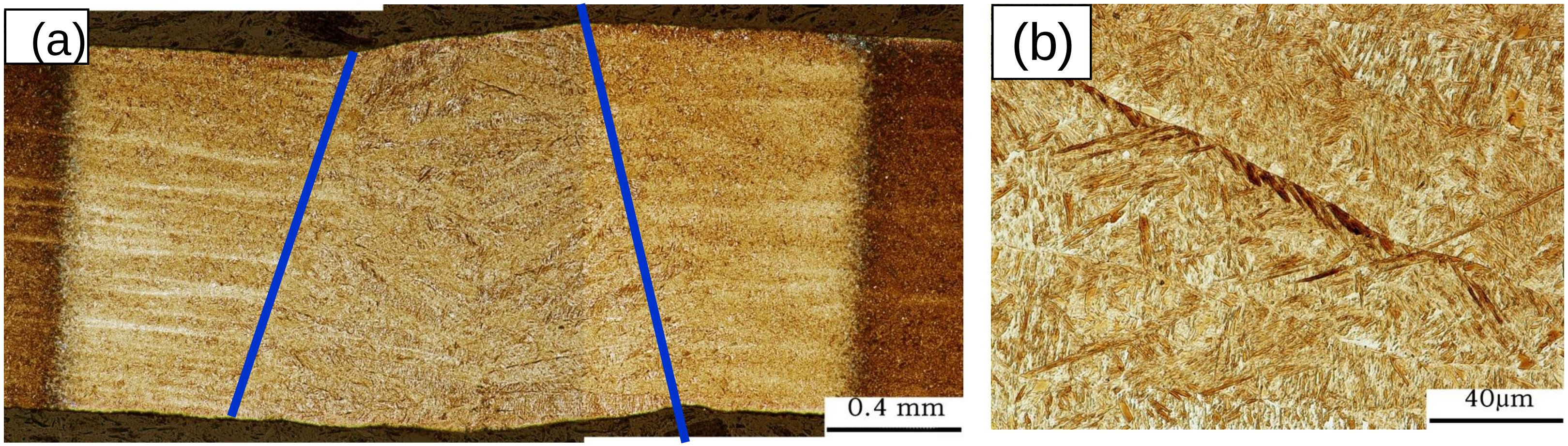

After QPT, 1800 MPa @ 14%El, **original**

Tensile strength of 1600MPa and elongation of 5-6% **after laser welding**.

Fracture toughness measurement

Three point bend SE(B)
Arc-shaped bend A(B)
Compact tensile C(T)
DENT test

- Ductile tearing resistance measured by the essential work of fracture (w_e)
- Critical crack Tip Opening Displacement (δ_c)
- Fracture toughness at cracking initiation(J_{IC})
- Linear-Elastic Plane-Strain Fracture Toughness KIC

ASTM E399-09, A. (2009). "Standard Test Method for Linear-Elastic Plane-Strain Fracture Toughness KIC of Metallic Materials."
ASTM E1290-08, A. (2008). "Standard Test Method for Crack-Tip Opening Displacement (CTOD) Fracture Toughness Measurement."

Transformation Induced Plasticity (TRIP) steel sheet with thicknessabout 1.4mm

DENT specimens for tensile test

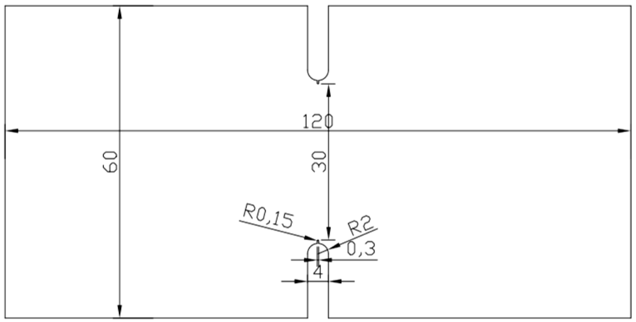

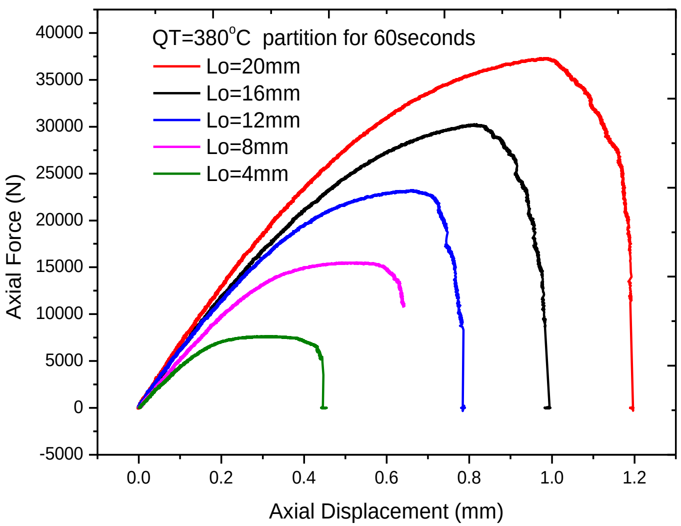

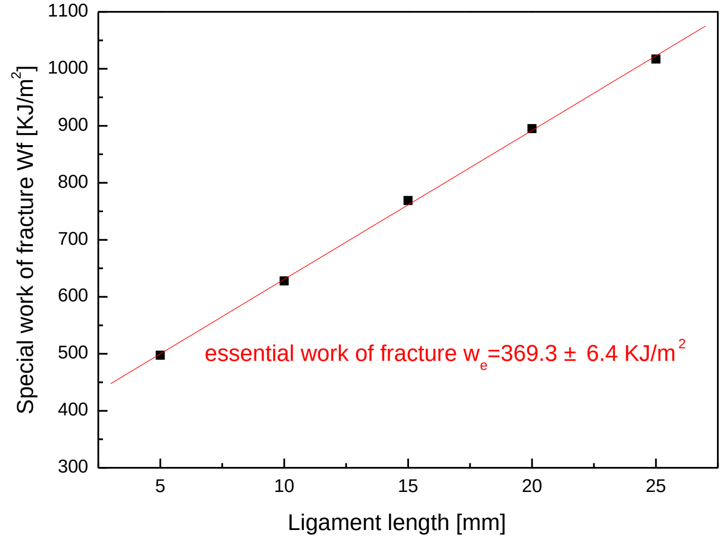

$$J = \mathcal{G} + \frac{1}{b}\left[2\int_0^{\delta_{\text{plastic}}} P d\delta_{\text{plastic}} - P\delta_{\text{plastic}}\right]$$

$$J_{\text{elastic}} = \mathcal{G} = \frac{K^2}{E}$$

Jacques, P., Q. Furnémont, et al. (2001). "On the role of martensitic transformation on damage and cracking resistance in TRIP-assisted multiphase steels." Acta Materialia 49(1): 139-152.

Knockaert, R., I. Doghri, et al. (1996). Experimental and numerical investigation of fracture in double-edge notched steel plates. International journal of fracture. 81: 383-399.

Transformation Induced Plasticity (TRIP) steel sheet with thicknessabout 1.4mm

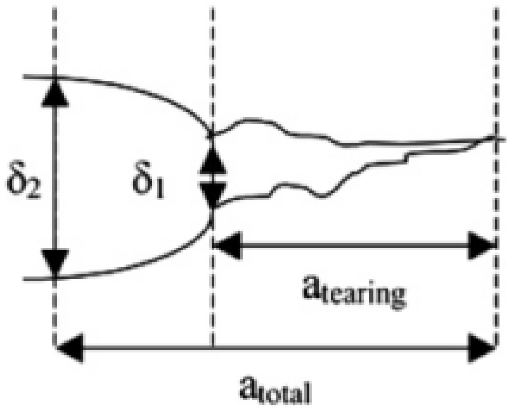

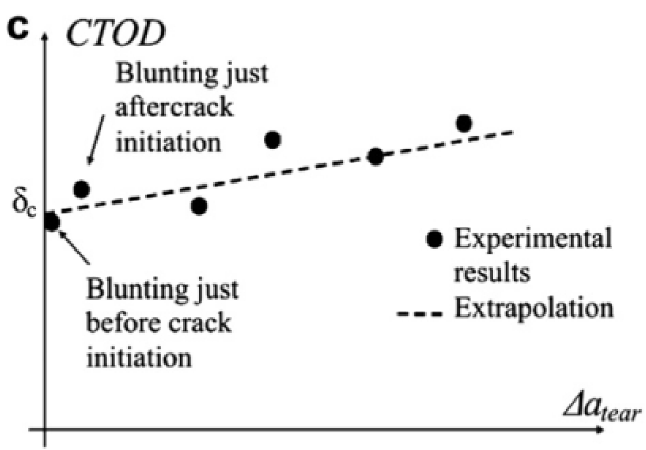

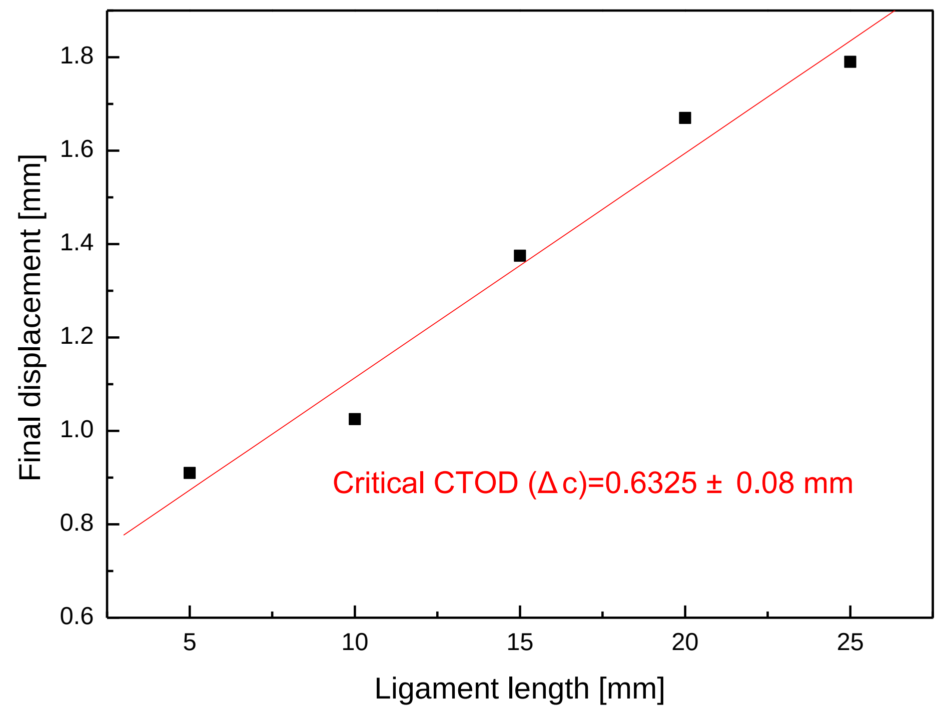

$$d_{\mathrm{final}} = \Delta_c + \theta l_0$$

Knockaert, R., I. Doghri, et al. (1996). Experimental and numerical investigation of fracture in double-edge notched steel plates. International journal of fracture. 81: 383-399.

Q&P Properties

PT-time °C-s	UTS MPa	YS MPa	EL %	w_e $KJ.m^{-2}$	J_{IC} $KJ.m^{-2}$	δ_C μm
			TRIP 780	369.3	?	632
260-60	1485.37	1021.92	7.8	329±31	136±56	327±15
280-60	1339.82	892	9.2	317±27	182±41	382±8
300-60	1220.05	858.5	11.54	424±31	268±39	552±11
320-60	1296.58	920.48	13.2	**451±26**	**283±35**	**699±6**
340-60	1314.79	901.03	12.52			
360-60	1239.72	875.48	12.34			
380-60	1208.6	903.27	10.09			

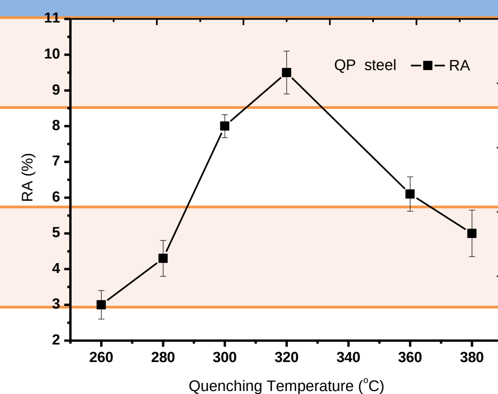

QP240ºC-60S

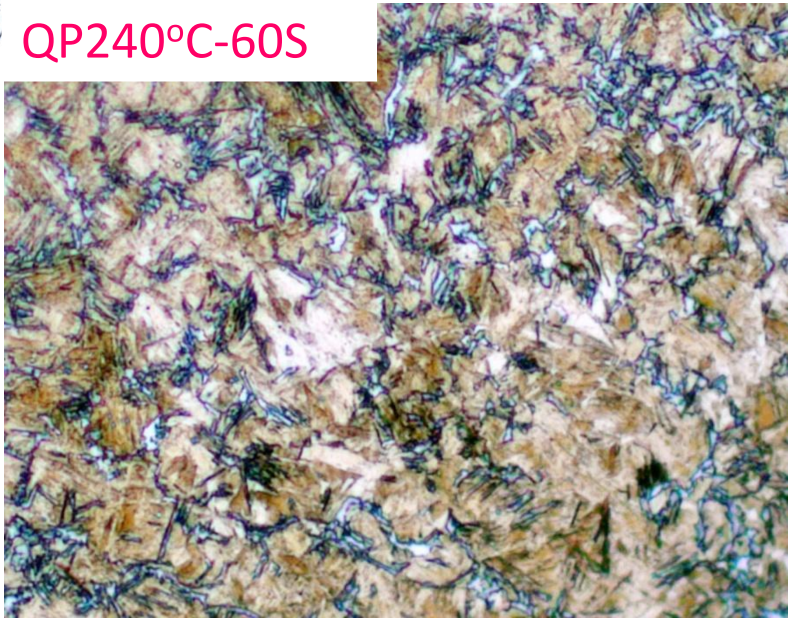

QP260ºC-60S

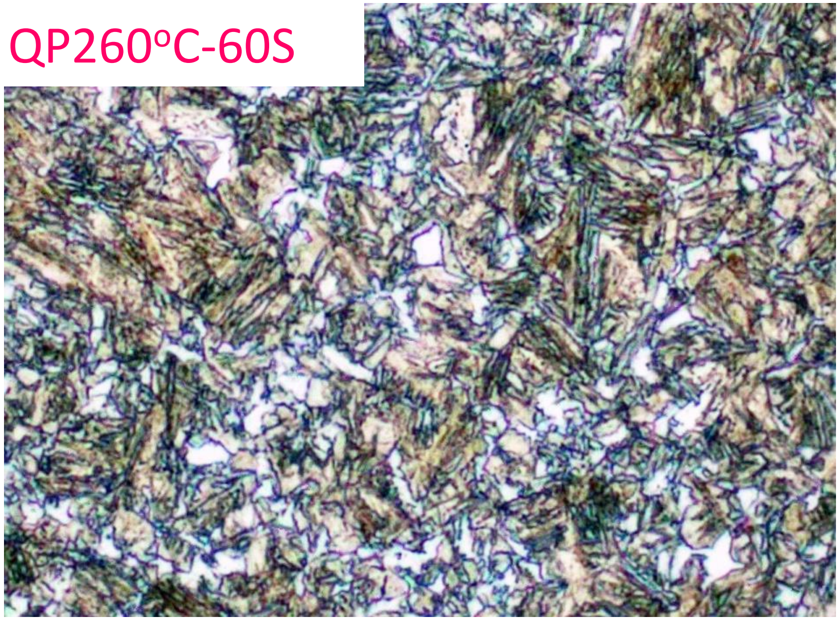

QP280ºC-60S

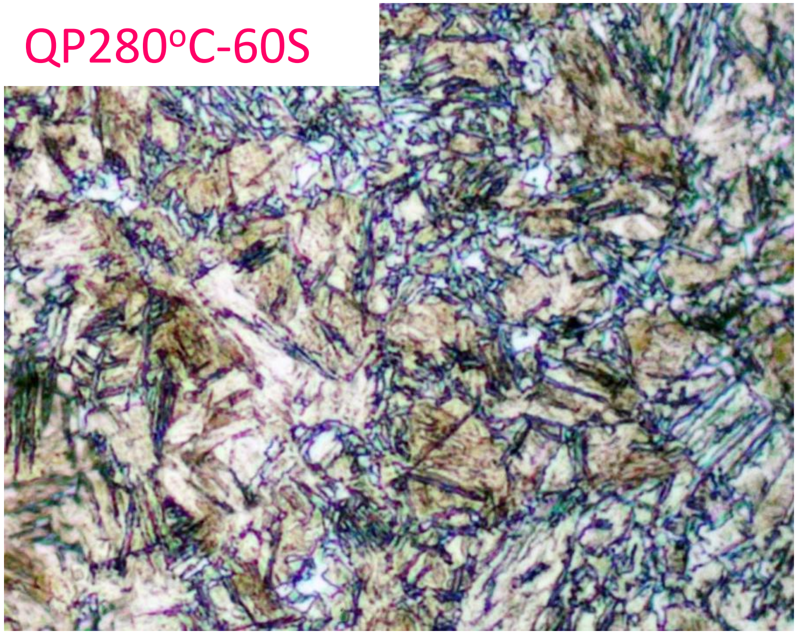

QP300ºC-60S

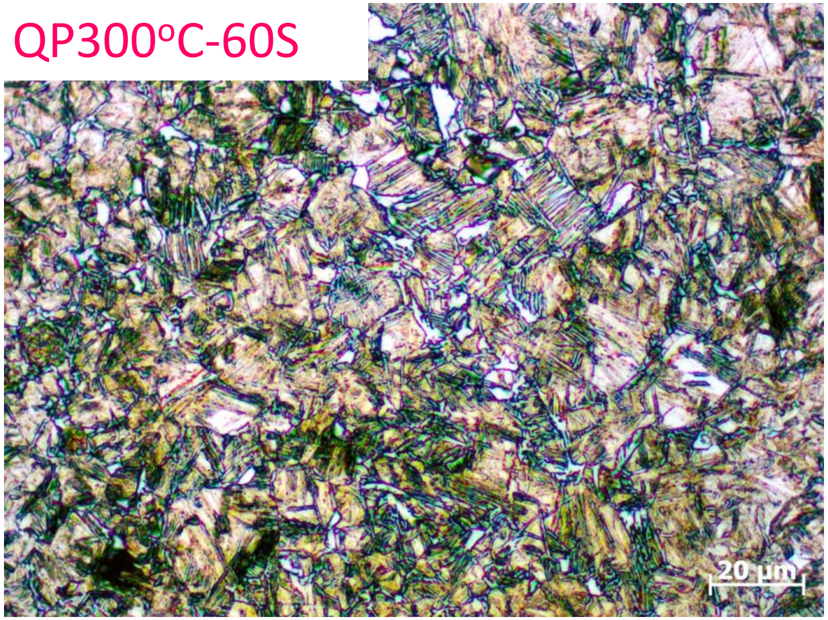

Q&P steel QT=320^{o}C for 60 seconds

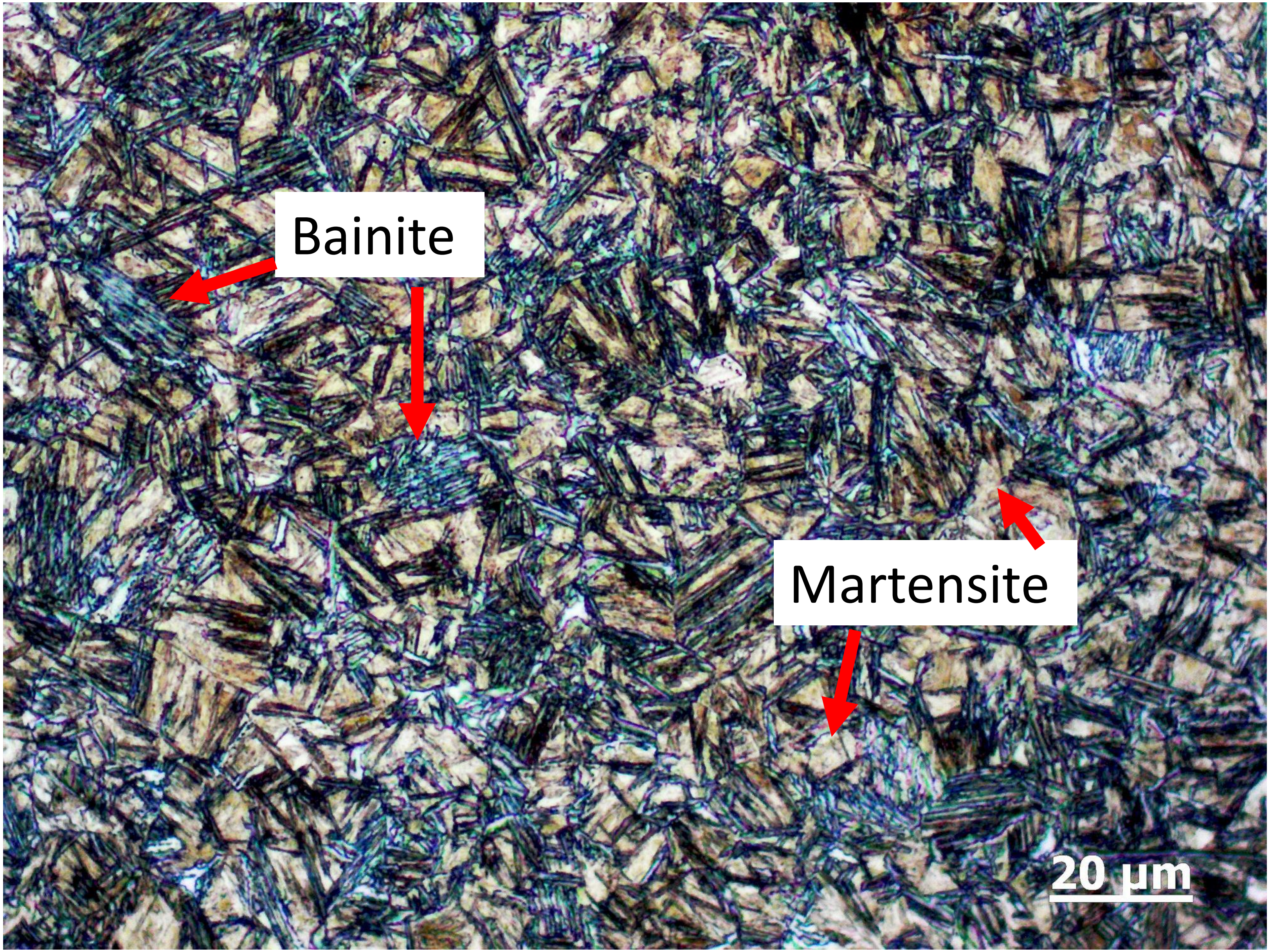

Fractography

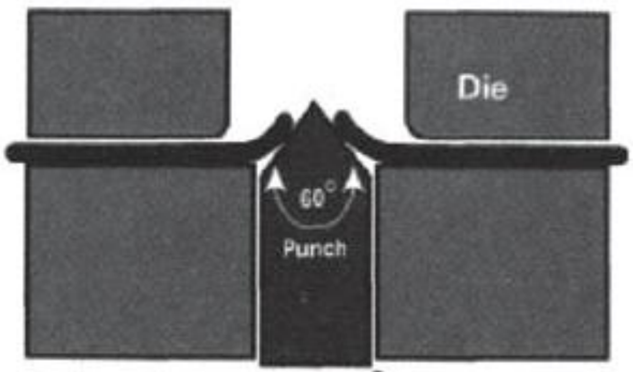

Hole expansion

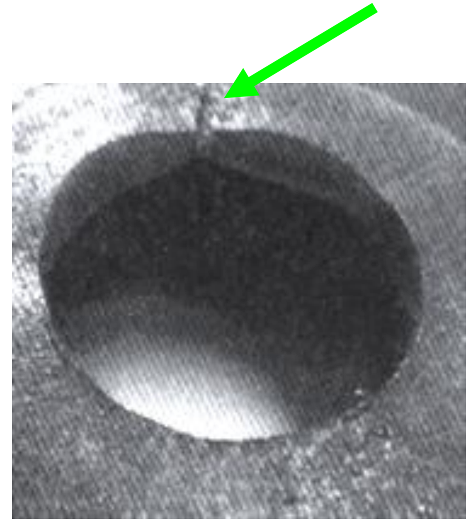

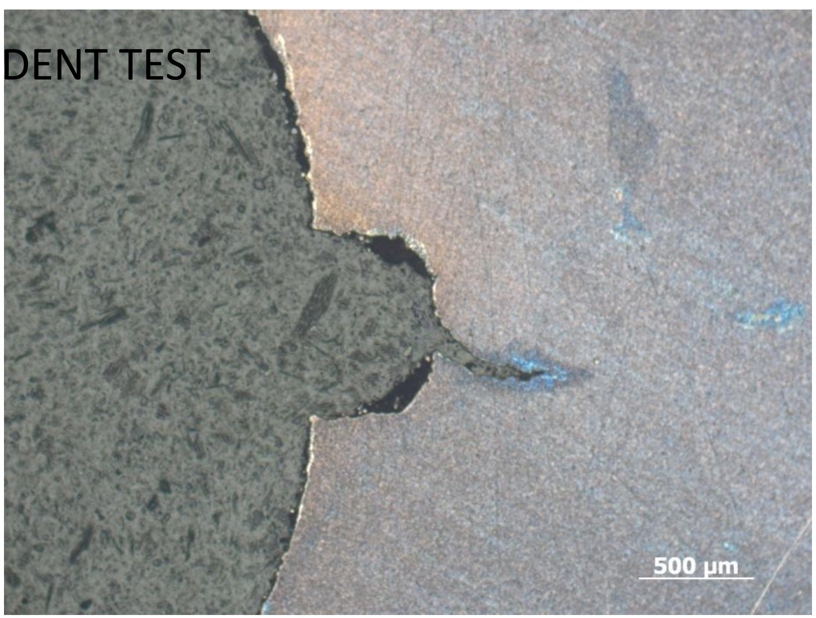

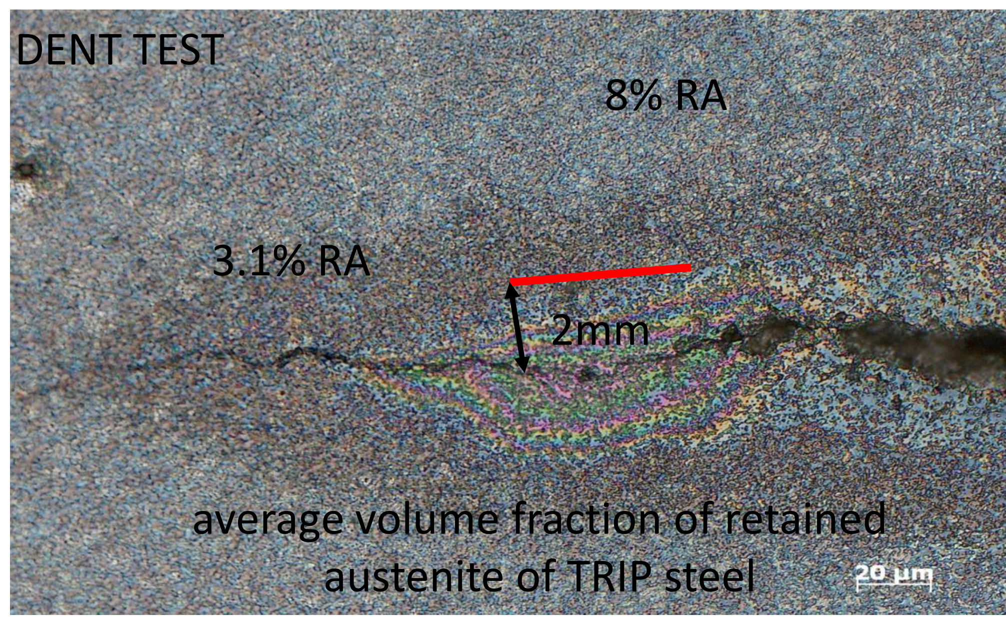

Charles, Y., et al., *Modelling the competition between interface debonding and particle fracture using a plastic strain dependent cohesive zone.* Engineering Fracture Mechanics, 2010. **77**(4): p. 705-718.

OUTLINE

- Introduction
- Quenching and Partitioning Treatment
  – Processing and Alloying
  – Microstructure and properties
  – Competing Process and Kinetics Models
    - Carbide formation and suppression
    - Migration of the martensite/austenite interface
    - Carbon partitioning and partitioning kinetics
- Combination of QPT with Hot Stamping and Application Concerns
- **Unsolved Issues**
- Concluding remarks

Unsolved Issues

1. Quantitative modeling for work hardening of multi-phase steels correlated with TRIP effect
2. Strategy of designing/selecting process with proper alloying for automobile
3. Kinetics of competing processes

1. Quantitative modeling for work hardening of multi-phase steels

- TRIP-assisted: how quantitatively to evaluate cooperative effect of multi-phase
- Work hardening: how to optimize plastic deformation and transformation in order to beat necking
- Length scale / multi-scale
  - Precipitation VS effective grain or sub-grain size
  - Toughness VS strength

Deformation induced martensitic transformation and transformation induced plasticity

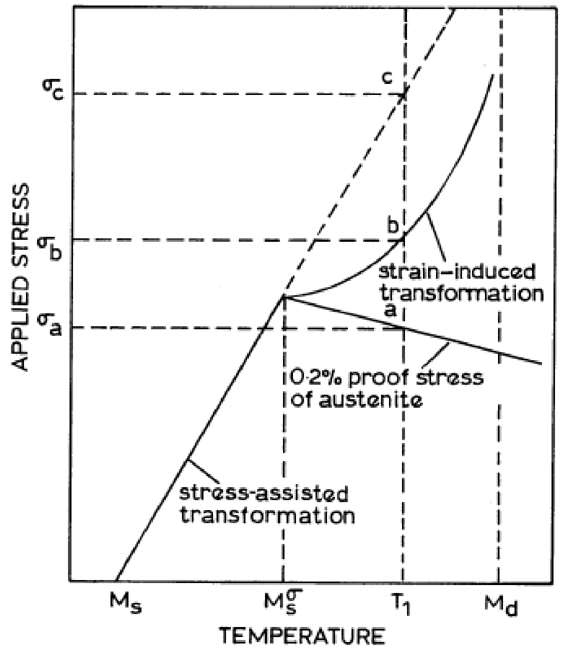

3 Schematic illustration showing critical stress for martensite formation as function of temperature

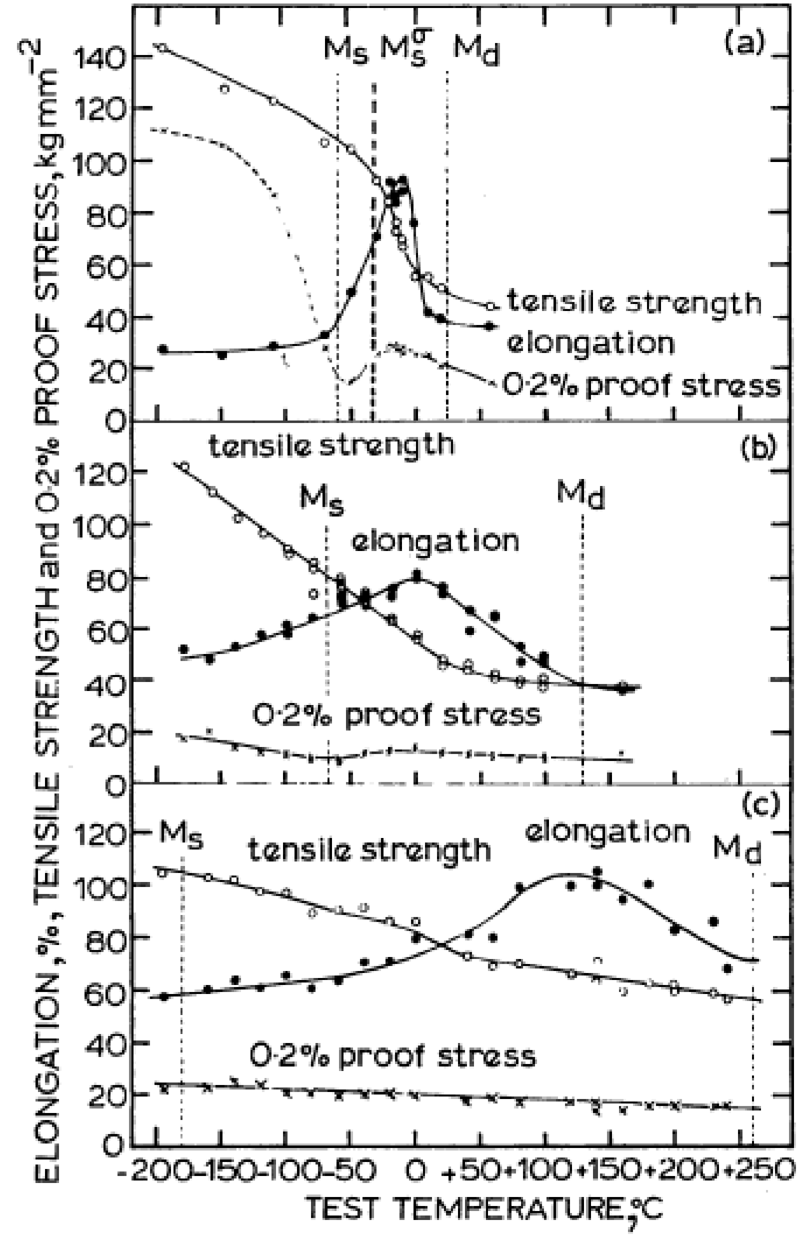

a Fe–29Ni–0·26C; *b* Fe–19Cr–11Ni; *c* Fe–24Mn–0·26C

- **Martensite morphology (lath or epsilon)**
- **Stability of austenite**
- **Temperature difference between Ms and Md with Ms(sigma) just below ambient**

I. Tamura
Metal Science Vol. 16 May 1982 245

TRIP effect for multi-phase system

- 15% * 0.15 = 2.25% directly from TRIP effect
- In addition to plastic deformation and TRIP effect, cooperative interaction between different phases may take effect !
- Partition of stress and strains

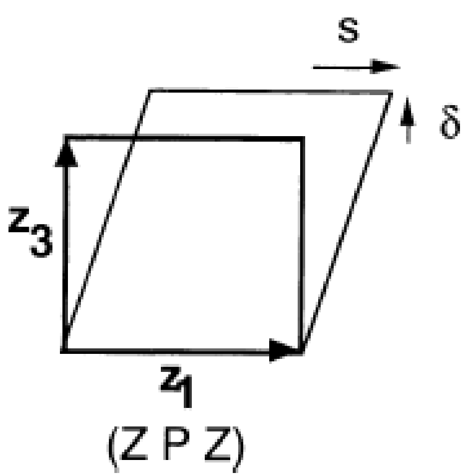

In a tensile test the effect of constraint due to the grips is to cause the sample to rotate [*e.g.* Ref. 5)] making $\mathbf{v}\|\mathbf{u}$ so that the net strain along the tensile axis is given by

$$1-|\mathbf{v}|/|\mathbf{u}|=0.15$$

Fig. 1. An invariant–plane strain with a shear s and dilatation δ. The coordinates z_i represent an orthonormal set in which z_3 is normal to the invariant-plane and z_1 is parallel to the shear direction. (Z P Z) is the deformation matrix describing the strain.

H. K. D. H. BHADESHIA
ISIJ International, Vol. 42 (2002), No. 9, pp. 1059–1060

Work hardening

- Plastic deformation / pile-up of dislocations
- Harder martensite induced by deformation
- Optimize the stability to beat the necking where unstable plastic deformation takes place
  - Especially in the late stage during deformation
  - Md30, temperature where half of austenite has been transformed to austenite under 30% true deformation strain
  - Designing by composition, effective phase size, location, morphology, so on of retained austenite

Optimizing the stability of retained austenite

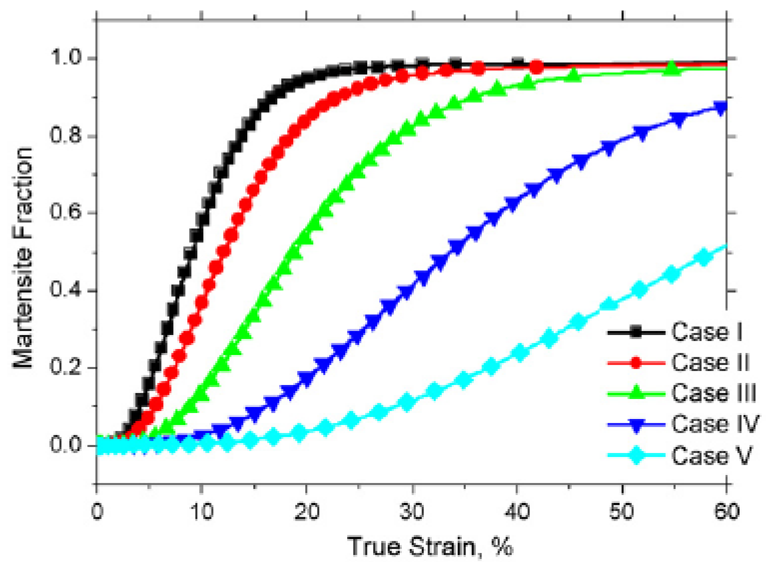

Fig. 3. Martensitic volume fraction mechanically transformed under various stability conditions of retained austenite corresponding to Table 2.

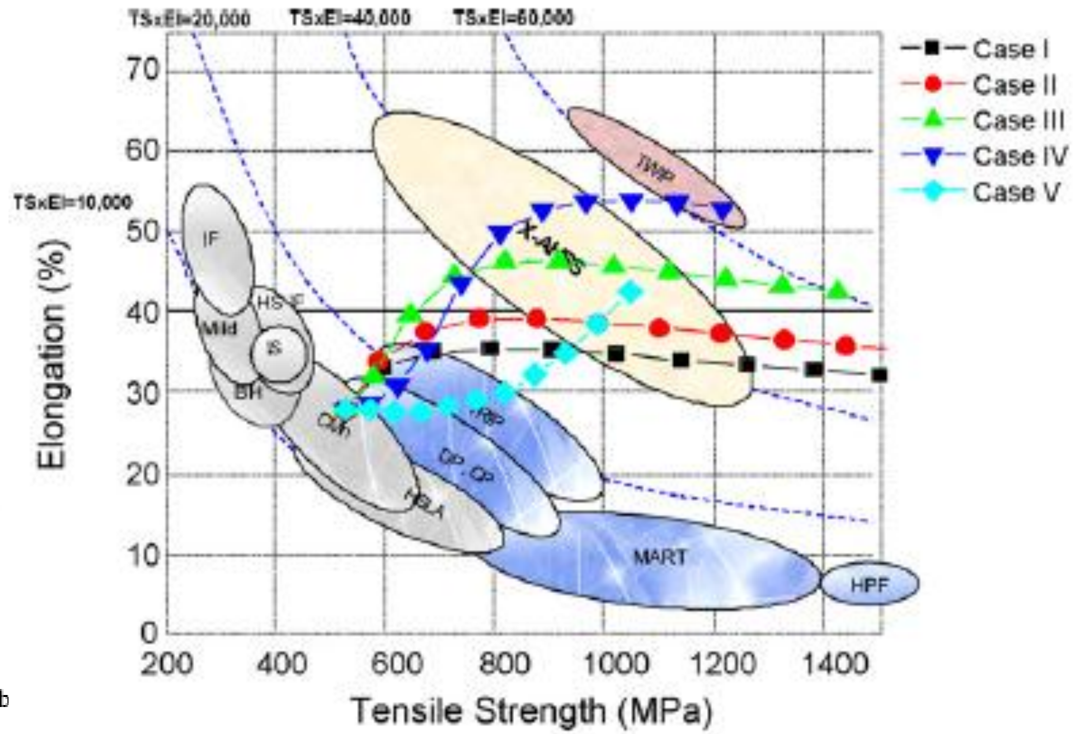

Fig. 9. A design application of TRIP-aided multiphase steel.

Modified rule of mixture with damage model

Heung Nam Hana,∗, Chang-Seok Ohb, Gyosung Kimc, Ohjoon Kwonc
Materials Science and Engineering A 499 (2009) 462–468

Acta metall. Vol. 31, No. 12, pp. 2037–2042, 1983
Printed in Great Britain

0001-6160/83 $3
Pergamon

EFFECT OF RETAINED AUSTENITE ON THE YIELDING AND DEFORMATION BEHAVIOR OF A DUAL PHASE STEEL

ANIL K. SACHDEV
Metallurgy Department, General Motors Research Laboratories, Warren, MI 48090–9055, U.S.A.

Table 1. Chemical analysis and average tensile properties of the dual-phase steel used in this study

Chemical analysis (wt.%)	
C	0.12
N	0.007
Mn	1.44
Si	0.50
V	0.061
Tensile properties	
Yield strength	367 MPa
Ultimate tensile strength	639 MPa
Uniform elongation	23%
Total elongation	32% (50 mm gage)

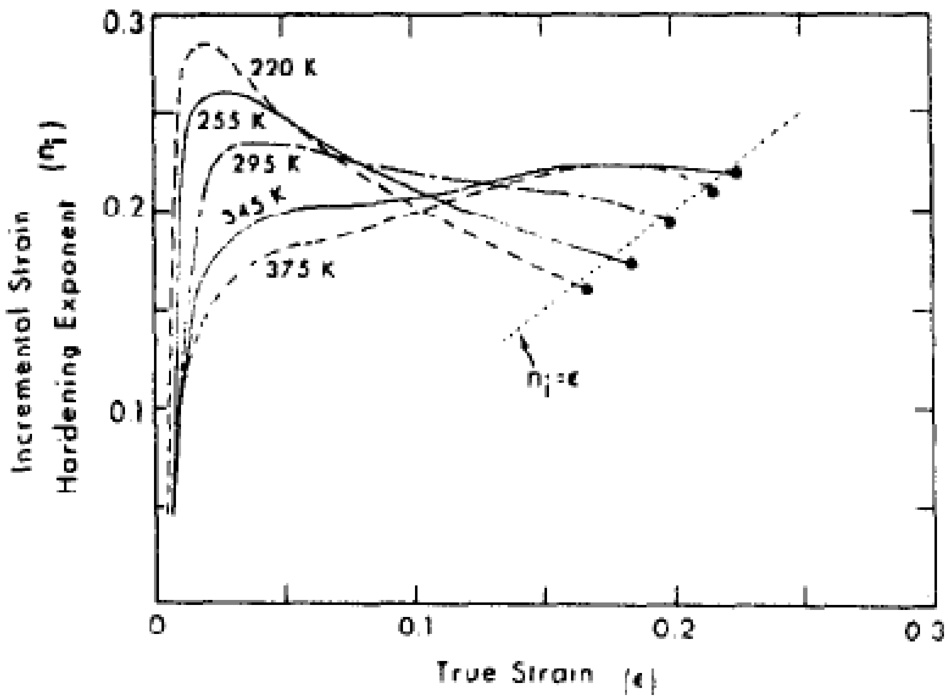

Fig. 3. Incremental strain hardening exponent (n_i) vs true strain for the various testing temperatures. The solid circles indicate the uniform elongation measured at the maximum tensile load.

Mn-Duplex stainless TRIP steels with 1GPa@60%

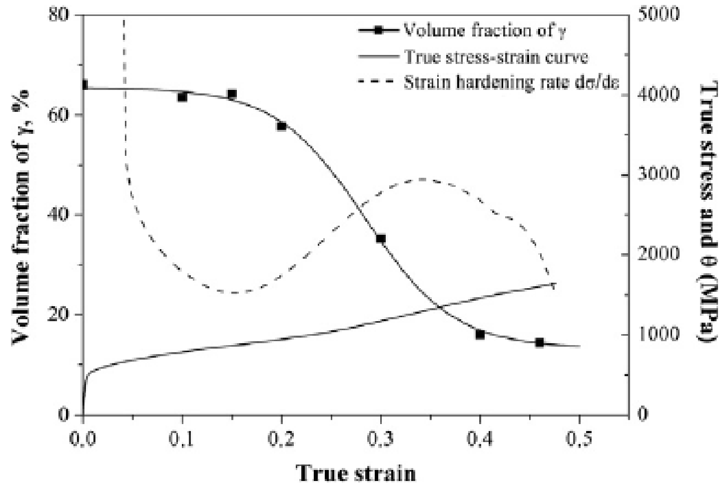

(Fe-19.9Cr-0.42Ni-0.16N-4.79Mn-0.11C-0.46Cu-0.35Si, wt.%)
Hot-rolling + Cold-rolling + Recrystalinzation

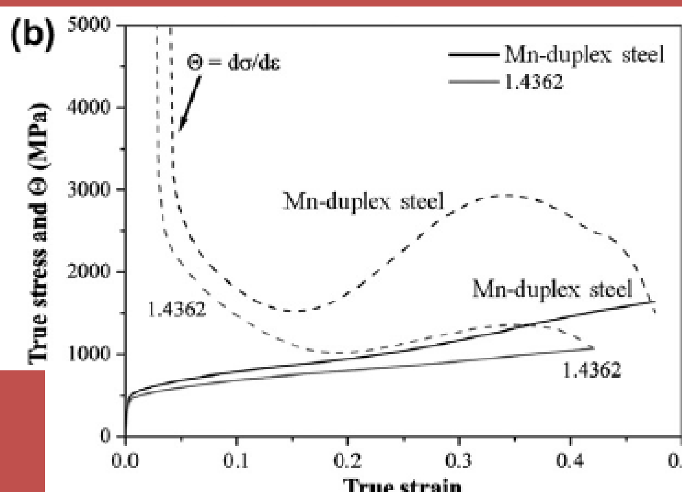

Md_{30}=64.0 C

28.1C for 1.4362

$$Md(\gamma) = 551 - 462(C(\gamma) + N(\gamma)) - 9.2Si(\gamma) - 8.1Mn(\gamma) - 13.7Cr(\gamma) - 29Ni(\gamma) - 29Cu(\gamma) - 18.5Mo(\gamma)$$

C. Herrera, D. Ponge, D. Raabe
Acta Materialia 59 (2011) 4653–4664

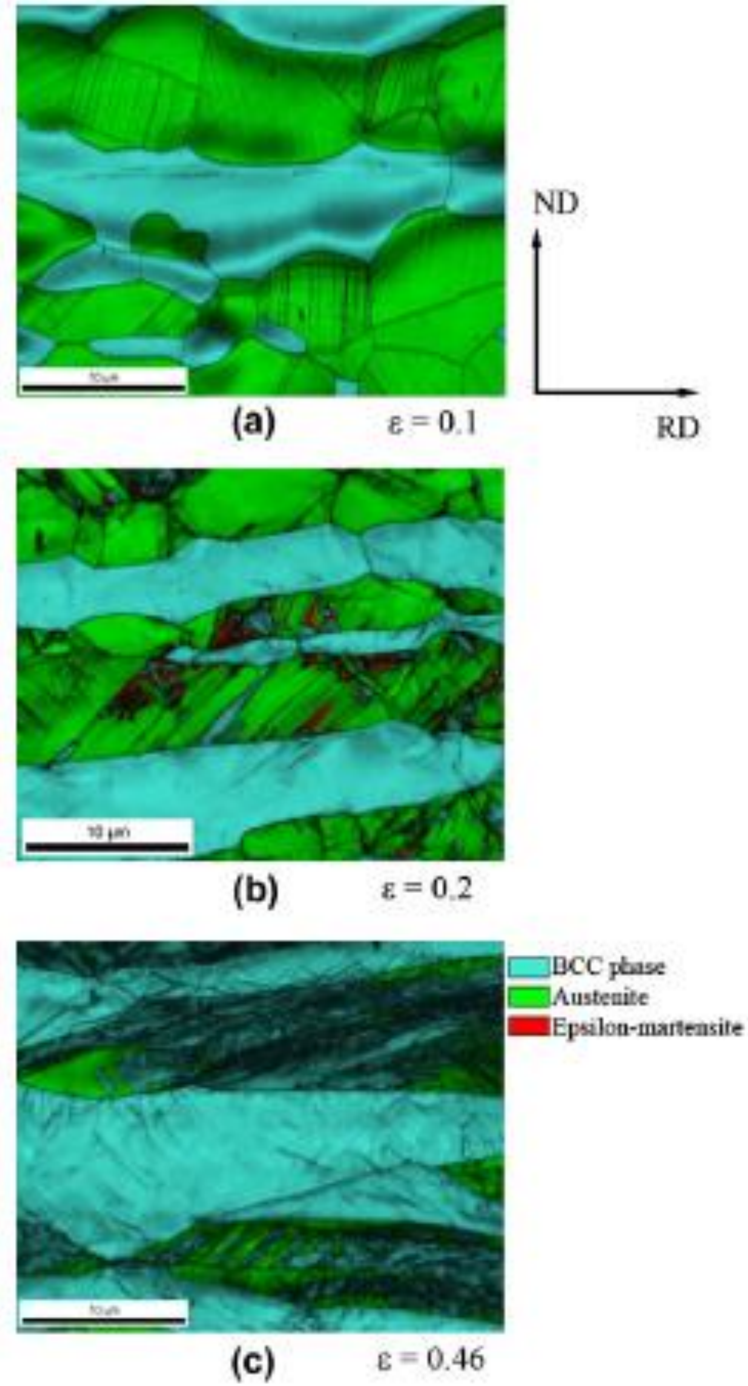

Alternative mechanisms of plasticity/toughness due to retained austenite beside to TRIP

- Blocking crack propagation， BCP

Webster D. Increasing the toughness of the martensitic stainless steel AFC77 by control of **retained austenite** content, ausforming and strain aging. Transactions of the ASM, 1968, 61(4):816-828.

- Dislocation absorption by retained austenite， DARA

Zhang K, Zhang M H, Guo Z H, et al. A new effect of **retained austenite on ductility enhancement** in high-strength quenching-partitioning-tempering-martensitic steel. Materials Science and Engineering A, 2011, 528: 8486- 8491.

Table 4.1 Microstructure parameters of martensite and retained austenite in tensile samples at different strain stages after the Q-P-T treatment

Strain	$(\varepsilon_M^2)^{1/2}$ ($\times 10^{-3}$)	ρ_{M1}	ρ_{M2}	$\overline{\rho}_M$ ($\times 10^{14}$ m^{-2})	$(\varepsilon_A^2)^{1/2}$ ($\times 10^{-3}$)	ρ_{A1}	ρ_{A2}	$\overline{\rho}_A$ ($\times 10^{14}$ m^{-2})	V_{RA} (%)
0%	2.52±0.06	7.29±0.25	7.23±0.21	7.26±0.23	2.25±0.29	13.66±0.89	8.32±0.71	10.99±0.80	13.2
1%	2.36±0.06	7.01±0.23	6.24±0.18	6.63±0.21	2.53±0.25	16.46±1.32	20.83±1.44	18.65±1.38	11.3
3%	2.24±0.07	5.82±0.23	6.13±0.23	5.98±0.23	3.07±0.37	27.29±2.88	26.65±2.69	26.97±2.79	8.2
5%	2.19±0.09	5.86±0.26	5.55±0.24	5.71±0.25	3.42±0.44	37.31±3.20	30.56±3.43	33.94±3.32	5.5
7%	2.29±0.08	6.46±0.25	6.00±0.27	6.23±0.26	3.71±0.45	39.86±4.21	42.19±4.50	41.03±4.36	4.2

how quantitatively to evaluate cooperative effect of multi-phase

2. Strategy of designing/selecting process with proper alloying for **automobile (AHSS)**

- DP
- TRIP
- TWIP
- QP

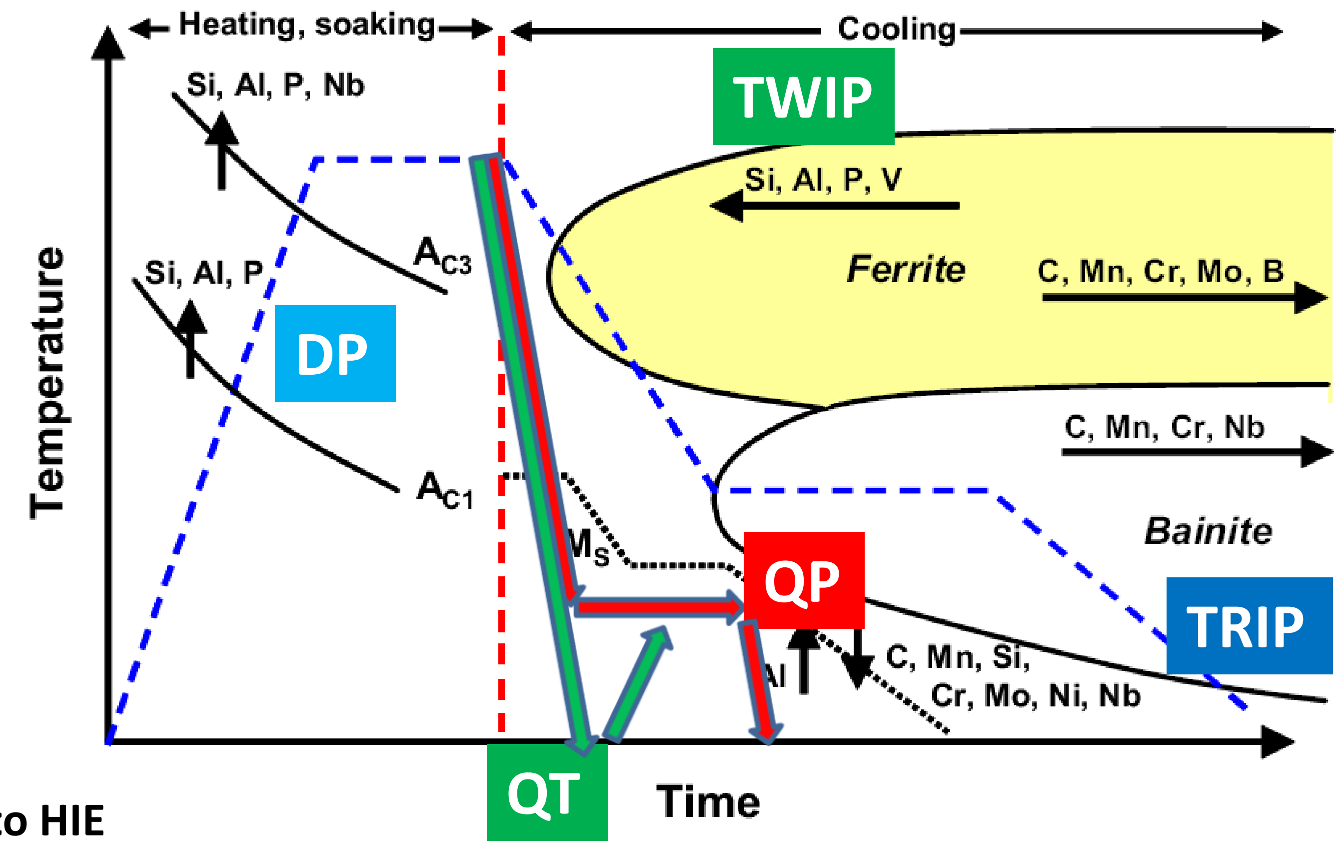

- **Cost**
- **Formability**
- **Weldability**
- **Susceptability to HIE**

Microstructure of
Metastable Multi-scale Multi-phase

- Composition
- Processing

Bleck, W. and K. Phiu-On, *Effects of Microalloying in Multi Phase Steels for Car Body Manufacture.* Microstructure and Texture in Steels, 2009: p. 145-163.

Suwas, S., A. Bhowmik, and S. Biswas, *Ultra-fine Grain Materials by Severe Plastic Deformation: Application to Steels.* Microstructure and Texture in Steels, 2009: p. 325-344.

Development in Multi Phase Steels for Car Body Manufacture

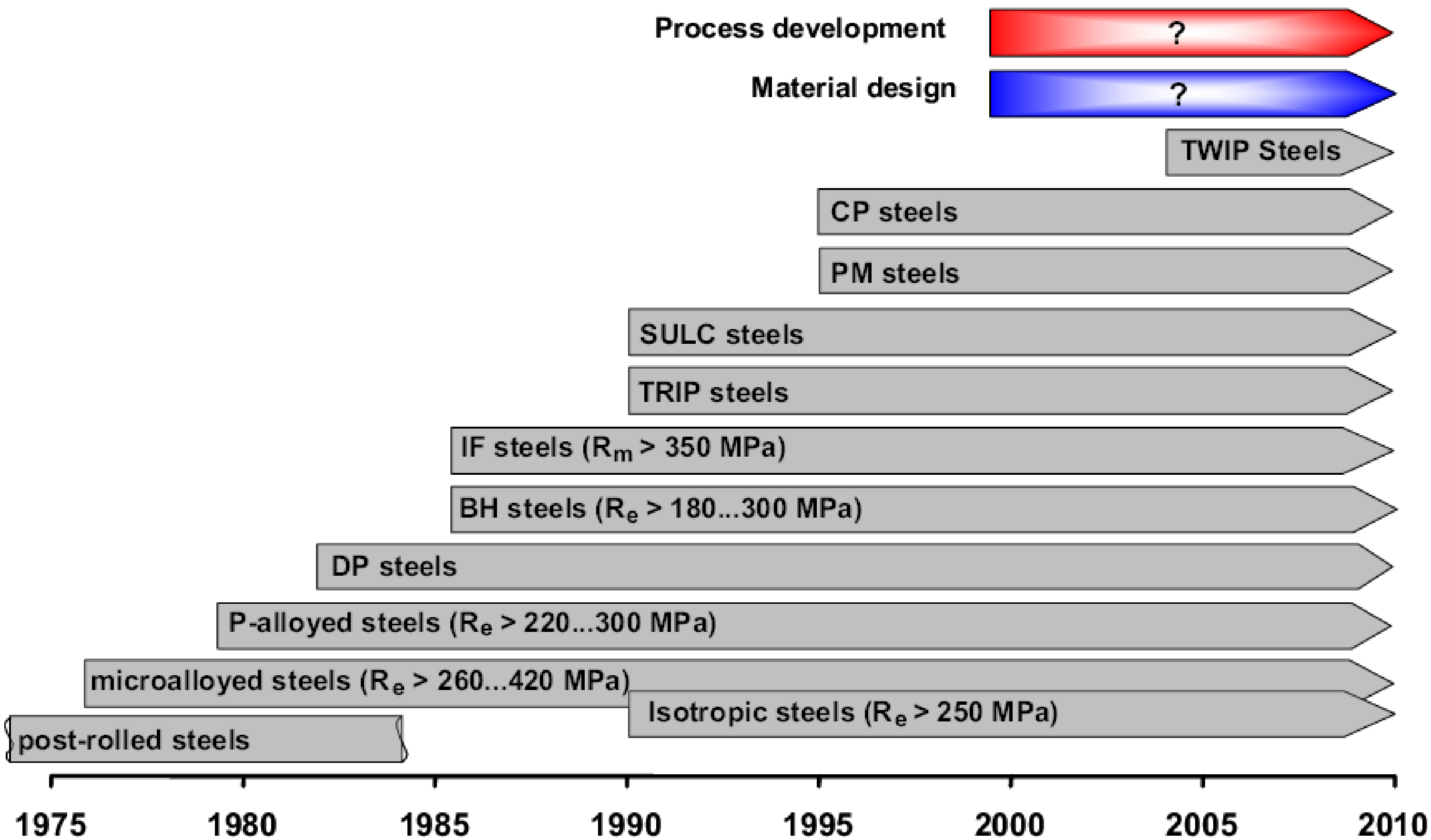

Bleck, W. and K. Phiu-On, *Effects of Microalloying in Multi Phase Steels for Car Body Manufacture.* Microstructure and Texture in Steels, 2009: p. 145-163.

Suwas, S., A. Bhowmik, and S. Biswas, *Ultra-fine Grain Materials by Severe Plastic Deformation: Application to Steels.* Microstructure and Texture in Steels, 2009: p. 325-344.

Toughness
Weldability
Susceptibility to hydrogen

- Sheet
- Multi-phase
- Deformation induced transformation from austenite to martensite

Available online at www.sciencedirect.com
SciVerse ScienceDirect
ELSEVIER
Acta Materialia 60 (2012) 4085–4092
Acta MATERIALIA
www.elsevier.com/locate/actamat

Effect of deformation on hydrogen trapping and effusion in TRIP-assisted steel

Joo Hyun Ryu [a], Young Soo Chun [c], Chong Soo Lee [c], H.K.D.H. Bhadeshia [a,b], Dong Woo Suh [a,*]

[a] *Graduate Institute of Ferrous Technology, POSTECH, Republic of Korea*
[b] *Materials Science and Metallurgy, University of Cambridge, Cambridge, UK*
[c] *Materials Science and Engineering, POSTECH, Republic of Korea*

Received 30 January 2012; received in revised form 3 April 2012; accepted 7 April 2012
Available online 18 May 2012

3. Kinetics of competing processes

- Decomposition of austenite
  - Precipitation
  - Bainite reaction
- Thermodynamically // Kinetically

A few processes concurrently take place at medium temperature for lean composition such as partitioning, precipitationand bainitic reaction et al.

2) Carbon partitioning from martensite to austenite

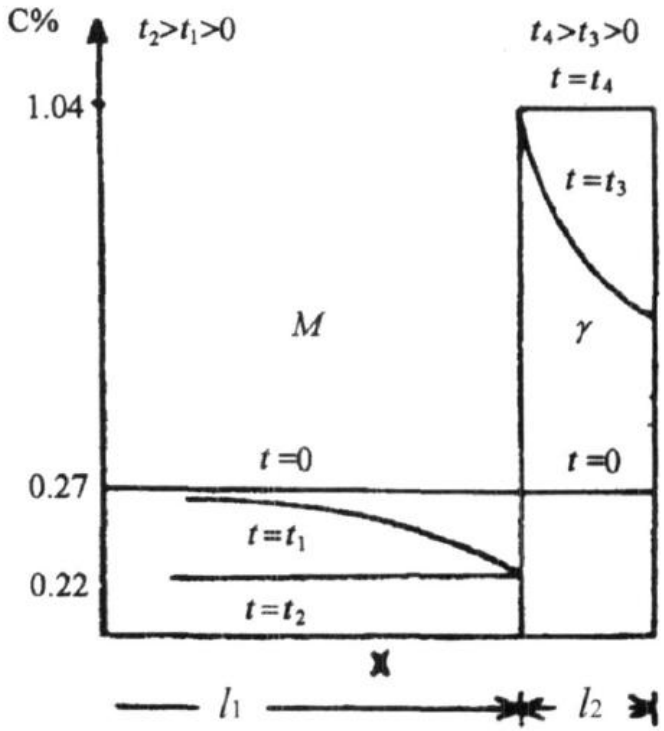

Figure 1 Sketch of carbon concentration profile in martensite and retained austenite for quenched 0.27%C steel

1979, *Thomas et. al*   *Hsu and Li* in 1983

By comparison the calculated durations between the formation of lath martensite and carbon partitioning owing to the different solubility of carbon in martensite and austenite, with carbon concentration profile as shown in Figure 1, *Hsu and Li* in 1983 showed that the carbon partition may keep pace with, or slightly lag behind, the formation of lath martensite. The time required for equalization of enriched austenite is at least one order of magnitude slower than the formation of lath martensite.

3) Kinetics for an athermal martensitic transformation

Koistinen and Marburger; *Magee*: kinetics equation for an athermal martensitic transformation

$$f=1-exp[-\alpha(M_s-T_q)] \qquad (1)$$

where $\alpha=1.10\times10^{-2}$ for carbon content 0.37 to 1.10mass%.

ΔG is a function of not only temperature but also the carbon content in austenite and the Magee's equation, or the Koistinen and Marbarger equation should be modified.

$$f=1-exp[\beta(c_2-c_1)-\alpha(M_s-T_q)] \qquad (2)$$

where , c_2 and c_1 represent the carbon contents in austenite before and after quenching.

---

[49] Hsu TY(Xu Zuyao), Lu W, Wang Y(1995) Influence of rare earch on martensitic transformation in a low carbon steel. Iron and Steel 30(4):52-58(in Chinese).
[50] Hsu TY(Xu Zuyao)(eds)(1999) Martensitic Transformation and Martensite(2nd Ed). Science Press, Beijing, pp563, 1999

Modified Koistinen-Marburger Equation

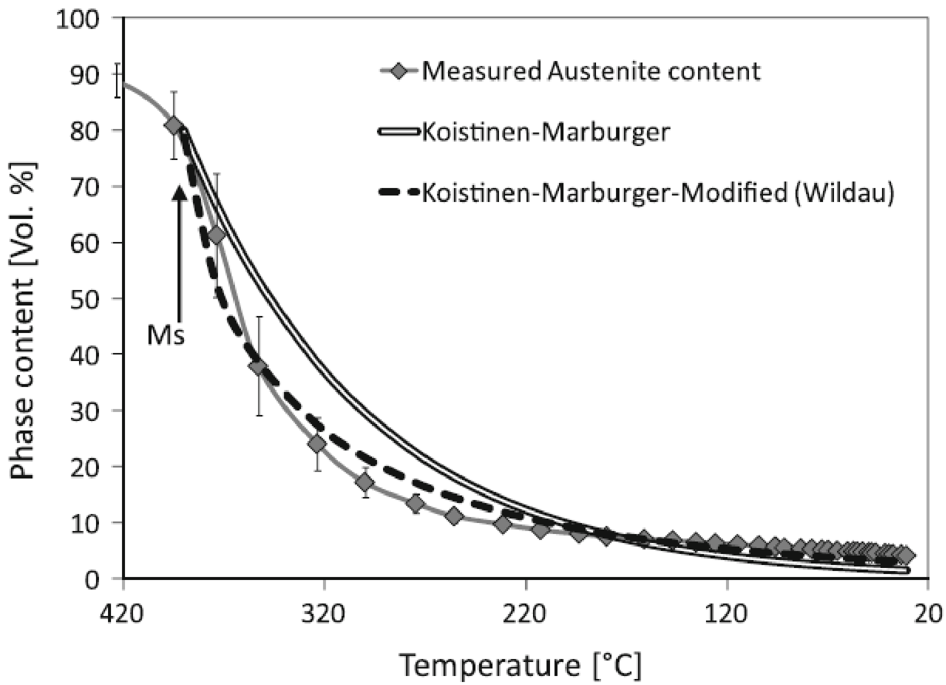

Fig. 11—Experimentally determined martensite transformation kinetic as well as modeled kinetic by the Koistinen-Marburger equation and by a modification of this equation.

Koistinen-Marburger equation

b = 0.011

$$V_A = A \times \exp[-b(Ms - Tq)]$$

Koistinen-Marburger modified by Wildau [3]

b = 0.011

n = 0.663

$$V_A = A \times \exp[-b(Ms - Tq)^n]$$

1 D.P. Koistinen and R.E. Marburger: Acta Metall., 1959, vol. 7, pp. 59–60.

2 S.-H. Kanga and Y.-T. Imb: J. Mater. Proc. Tech., 2007, vol. 183, pp. 241–44.

3 M. Wildau: Ph.D. Dissertation, Technical University of Aachen, Aachen, Germany, 1986.

4 J. Epp, T. Hirsch, and C. Curfs, Metall Mater Transact A 2012, vol. 43, pp. 2210-2217.

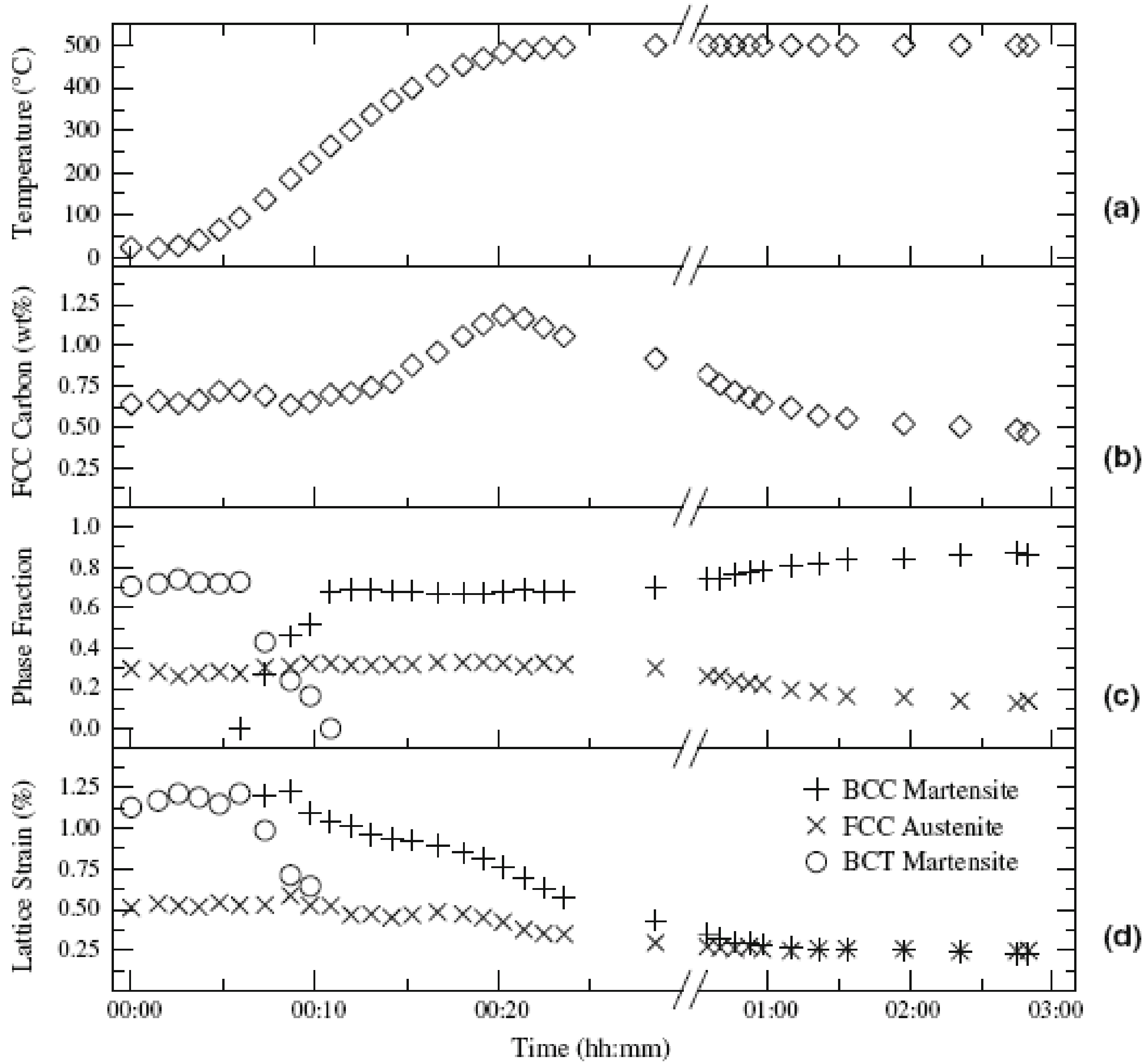

Fig. 12—*In situ* neutron diffraction results during heating (partitioning) of a 0.64C-4.57Mn-1.30Si steel after quenching to room temperature, showing phase fractions, austenite carbon concentration, and lattice strains.[56,57]

T.D. Bigg, D.K. Matlock, J.G. Speer, and D.V. Edmonds: Solid State Phenom., 2011, vols. 172–174, pp. 827–32.

Evidence from Internal friction

0.39C-1.56Si-2Mn-9.84Ni 730℃*30min+ water queching

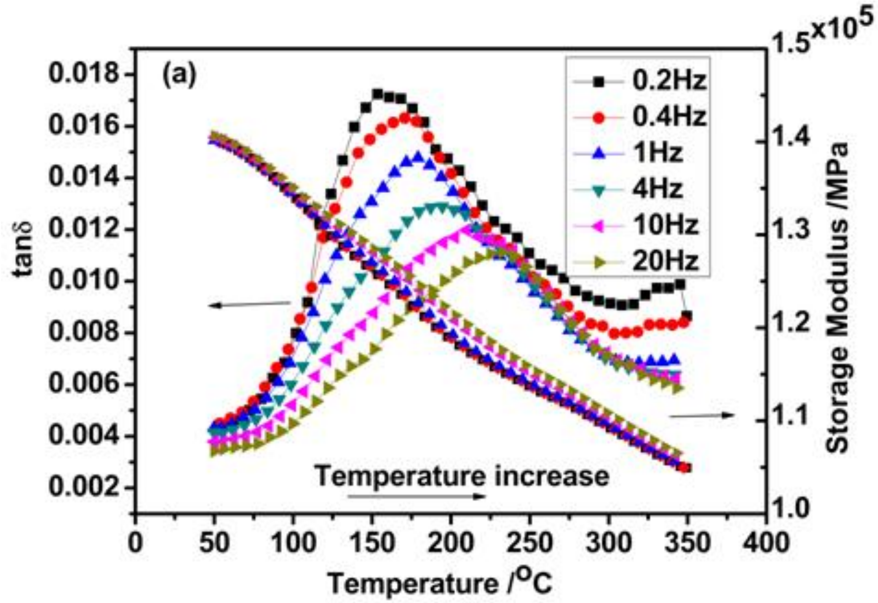

First heating curve (DMA)

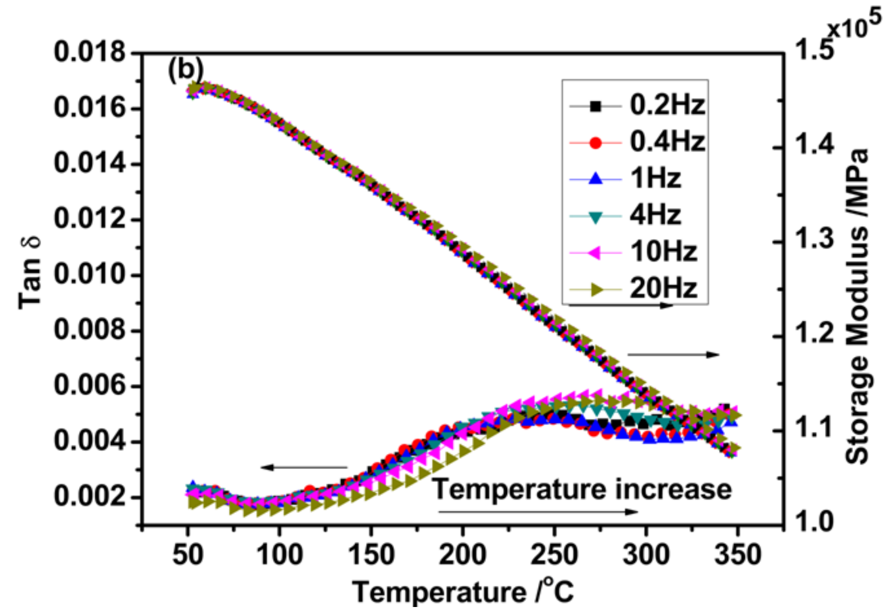

Second heating curve (DMA)

Interaction between carbon and dislocation

Activation energy 121KJ/mol (1.26eV)

Anelestic peaks

Temperature

Broaden peak

Snoek-köster-like anelestic peaks

resolving capability:

Internal friction 10^{-6}

DMA 10^{-4}

OUTLINE

- Introduction
- Quenching and Partitioning Treatment
  - Processing and Alloying
  - Microstructure and properties
  - Competing Process and Kinetics Models
    - Carbide formation and suppression
    - Migration of the martensite/austenite interface
    - Carbon partitioning and partitioning kinetics
- Combination of QPT with Hot Stamping and Application Concerns
- Unresolved Issues
- **Concluding remarks**

Conclusions

- **Ultimate tensile strength of >2000MPa and total elongation of >10%**, Microstructure in QPT steels generally contains **~5% retained austenite**, with considerable thickness trapped between fine lath martensite embedded with **dispersed complex carbides or η(θ) carbide**
- Preliminary results show that combination of QP with hot deformation can improve the mechanical properties of AHSS. **Enhanced mechanical properties** and the total elongation of the steel increases from 6.6% to 14.8% compared with that of hot stamped and quenched steel.
- A few unresolved issues such as the multi-phase modeling of TRIP-assisted mechanical properties, designing strategy of AHSS targeting for automobiles and kinetics of competing processes.


Phase Transformation Group @ SJTU
with a few friends in 2012


Shanghai Jiao Tong University